JGR Earth Surface

RESEARCH ARTICLE
10.1029/2021JF006387

The Role of Fluid Seepage in the Erosion of Mesozoic Carbonate Escarpments

Aaron Micallef[1,2], Charles K. Paull[3], Nader Saadatkhah[1], and Or Bialik[2]

[1]Helmholtz Centre for Ocean Research, GEOMAR, Kiel, Germany, [2]Department of Geosciences, Marine Geology and Seafloor Surveying, University of Malta, Msida, Malta, [3]Monterey Bay Aquarium Research Institute, Moss Landing, CA, USA

Key Points:

- Box canyon formation is a significant erosive process across carbonate escarpments
- Fluid seeping through joints can drive initiation and retrogressive evolution of box canyons via periodic block failure at the canyon head

Correspondence to:
A. Micallef,
amicallef@geomar.de

Citation:
Micallef, A., Paull, C. K., Saadatkhah, N., & Bialik, O. (2021). The role of fluid seepage in the erosion of Mesozoic carbonate escarpments. *Journal of Geophysical Research: Earth Surface*, *126*, e2021JF006387. https://doi.org/10.1029/2021JF006387

Received 7 AUG 2021
Accepted 26 OCT 2021

Author Contributions:
Conceptualization: Aaron Micallef, Charles K. Paull
Formal analysis: Aaron Micallef, Charles K. Paull
Funding acquisition: Aaron Micallef
Methodology: Aaron Micallef, Charles K. Paull, Nader Saadatkhah
Resources: Aaron Micallef, Charles K. Paull
Software: Nader Saadatkhah
Supervision: Aaron Micallef
Validation: Aaron Micallef, Or Bialik
Visualization: Aaron Micallef, Nader Saadatkhah, Or Bialik
Writing – original draft: Aaron Micallef
Writing – review & editing: Charles K. Paull, Nader Saadatkhah, Or Bialik

Abstract Mesozoic submarine carbonate escarpments are erosional features that host box canyons, the formation of which had been attributed to seepage erosion in view of their similarity to subaerial box canyons. The latter had been cited as diagnostic of groundwater activity, although the efficacy of fluid seepage as an erosive agent in bedrock remains controversial. Here we use multibeam echosounder data from the Blake, Campeche, Malta and Florida Escarpments to demonstrate that box canyon formation is, in general, a significant process eroding carbonate escarpments. Numerical modeling based on parameters from the Florida Escarpment shows that box canyons can initiate and retrogressively evolve by fluid seeping via joints, which causes a reduction in rock strength due to fluid pressure and dissolution, resulting in periodic block failure at the canyon head. Box canyon elongation is promoted by an exponential distribution of joint density, an increase in joint density, joints oriented perpendicular and parallel to the escarpment, or an increase in the thickness of the flowing groundwater zone and slope gradient of the escarpment. The angularity of the canyon head decreases with a decrease in joint density and when joint density is uniform, whereas the canyon width is regulated by the extent of the joint set zone. Since the key factors contributing to box canyon formation along the Florida Escarpment appear to characterize the Blake, Campeche and Malta Escarpments, the groundwater model for box canyon formation should be applicable to these escarpments as well.

Plain Language Summary Submarine carbonate escarpments are cliffs of limestone and dolomite that form anomalously steep topography on the Earth's surface. Box canyons—wide canyons with steep walls and semi-circular heads—are a common feature in carbonate escarpments and they have been associated with groundwater seepage. In this study, we use seafloor depth information from four carbonate escarpments to show that box canyon erosion is a key process driving their evolution. Numerical modeling, on the other hand, suggests that fluid seeping in conditions similar to those of the Florida Escarpment can result in box canyon formation via periodic failure of the canyon head. Since these conditions at the Florida Escarpment can also be found in other escarpments such as the Blake, Campeche and Malta Escarpments, box canyon formation by groundwater seepage is likely a widespread geological process. The location of box canyons may suggest where fluid is seeping along escarpments and where specialized biological communities may be located. Box canyon formation is unlikely to pose a risk to coastal communities and offshore infrastructure.

1. Introduction

1.1. Carbonate Escarpments

Carbonate escarpments consist of thick, exposed sequences of limestone and dolomite deposited in carbonate banks or platforms between the Late Triassic and Late Cretaceous (Bryant et al., 1969; Dillon & Popenoe, 1988; Locker & Buffler, 1983; Paull, Freeman-Lynde, et al., 1990). Occurring on some passive continental margins, carbonate escarpments are characterized by anomalously steep topographies (maximum local slope gradients of >70°) and generally steepen with depth. The relief of carbonate escarpments, which tends to be in excess of 1 km, is the result of the combined effects of the initial elevation of former shallow water platforms, subsequent subsidence, and different sediment accumulation rates on the platform and adjacent basins (Bryant et al., 1969; Locker & Buffler, 1983; Scandone et al., 1981; Schlager, 1981; Schlager & Camber, 1986; Uchupi & Emery, 1968).

1.2. Erosive Processes in Carbonate Escarpments

A wide range of evidence suggests that carbonate escarpments are the product of erosional processes. Examples of lines of evidence include: (a) the strata exposed across carbonate escarpments are platform interior deposits (predominantly mudstones and wackestones) rather than high energy facies typical of modern platform edges (e.g., grainstone, boundstone or bafflestone), (b) the freshness and abraded texture of rocks exposed across the escarpment, (c) the low thickness of sediment cover and lack of Fe-Mn coatings on the escarpment face, (d) the abrupt termination of seismic reflections at escarpments, and (e) the occurrence of buried benches at the base of some escarpments, which have been interpreted as evidence of retreat by erosional undercutting (Dillon et al., 1987; Freeman-Lynde, 1983; Freeman-Lynde & Ryan, 1985; Kohl, 1985; Land et al., 1999; Paull & Dillon, 1980; Paull, Freeman-Lynde, et al., 1990; Schlager et al., 1984). The Blake Escarpment in the vicinity of the Blake Spur, for example, is thought to have retreated by up to 15 km since the Oligocene (Dillon et al., 1987; Paull & Dillon, 1980), whereas the southern Florida Escarpment may have retreated by up to 8 km in the last 100 Ma (Corso & Buffler, 1985; Freeman-Lynde, 1983; Paull, Freeman-Lynde, et al., 1990).

A range of physical, chemical and biological mechanisms are thought to have eroded carbonate escarpments since their formation. The most commonly cited mechanisms include gravity flows (Casero et al., 1984; Holmes, 1985; Lindsay et al., 1975; Micallef et al., 2019; Paull, Freeman-Lynde, et al., 1990; Twichell et al., 1996), submarine landslides (Brooks et al., 1986; Mullins & Hine, 1989; Paull, Twichell, et al., 1991), sub-lysoclinal dissolution (Dillon et al., 1985, 1987; Paull, Commeau, et al., 1991), bottom currents (Dillon et al., 1987; Land et al., 1999; Paull & Dillon, 1980; Twichell et al., 1996), bioerosion (Dillon et al., 1987; Land et al., 1999; Neumann, 1966; Sikes, 1984) and fluid seepage. Seepage erosion, in particular, has been proposed as a key process to explain the formation of box canyons—canyons with theater-shaped heads, steep walls, constant width, flat floors and low drainage densities—because they are inconsistent with gravity flow erosion (Nagihara, 1996; Paull & Neumann, 1987; Paull, Spiess, et al., 1990; Twichell et al., 1990). Such an inference is mainly based on the similarity of escarpment box canyons with subaerial box canyons, which have been cited as diagnostic of groundwater activity (Dunne, 1990; Russel, 1902). In bedrock in subaerial settings, the classic model for the formation of box canyons entails a valley headwall that lowers the local hydraulic head and focuses groundwater flow to a seepage face. Here, corrosion weakens the rock, leading to undermining, collapse and retreat of the canyon head (Dunne, 1980, 1990; Laity & Malin, 1985). The occurrence of faults is thought to increase permeability and enhance the rate of groundwater flow and erosion (Dillon et al., 1993; Twichell et al., 1990).

1.3. Knowledge Gaps

In subaerial settings, fluid seepage has been shown to unambiguously lead to the formation of box canyons only in unconsolidated sand to gravel sized sediments (Lapotre & Lamb, 2018; Lobkovsky et al., 2007; Micallef et al., 2021; Schumm et al., 1995). The efficacy of fluid seepage as an erosive agent in bedrock remains disputed, however, and there is no unambiguous example of a bedrock box canyon formed by seepage erosion (Lamb et al., 2006). The mechanisms and rates of seepage weathering and erosion processes in subaerial bedrock are poorly constrained, and it is still unclear how box canyon geometries are generated (Lamb et al., 2006, 2008). There are a number of reasons for these gaps in knowledge. Field observations and experimental simulations of box canyon formation in bedrock are complicated by the long timescales involved and the overprinting of surface erosion processes. Experimental and numerical analyses have been based on simplistic assumptions related to flow processes and hydraulic characteristics, and they rarely take into consideration geologic heterogeneities or weathering (e.g., Luo & Howard, 2008; Nagihara, 1996; Pelletier & Baker, 2011). Subaerial box canyons can also be formed by surface water erosion without the need of groundwater flow, for example, in substrate with stratigraphic contrasts and vertical joints, waterfall erosion by abrasion, and megaflooding (Amidon & Clark, 2015; Lamb et al., 2006, 2007, 2008, 2014; Ryan & Whipple, 2020; Scheingross & Lamb, 2017). In view of the above, a re-evaluation of the role of groundwater in eroding submarine escarpments is necessary.

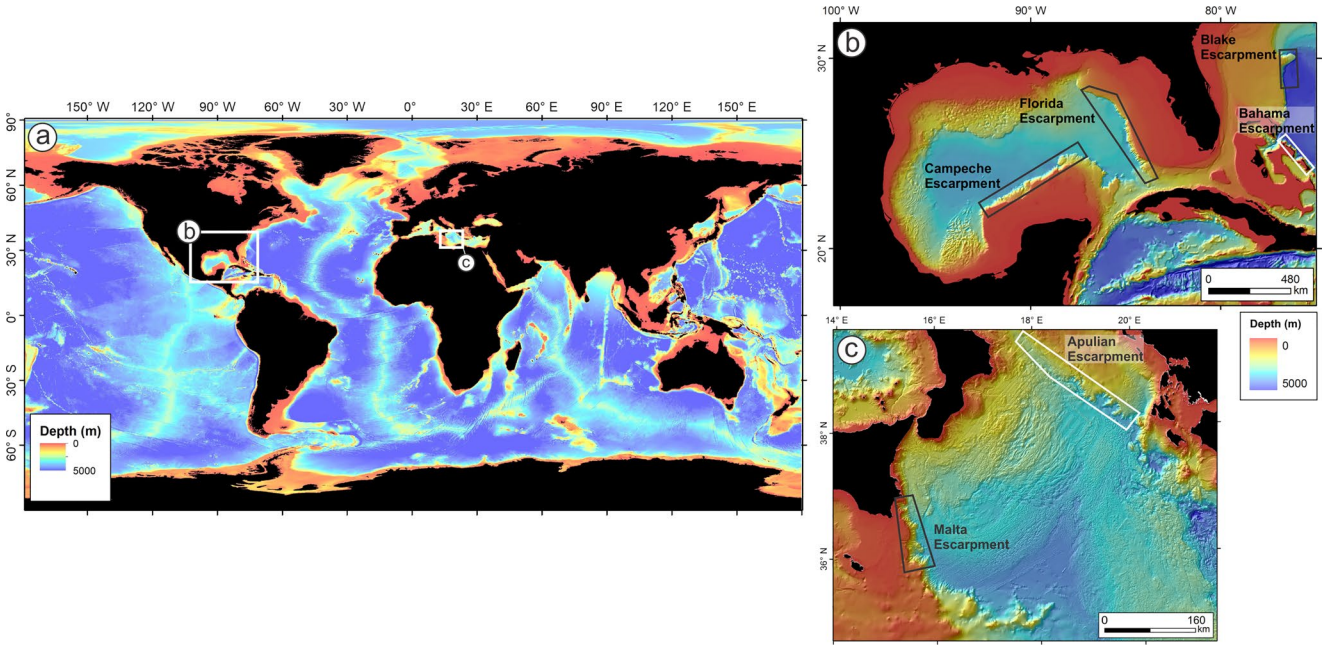

Figure 1. Location maps of the Apulian, Bahama, Blake, Campeche, Florida and Malta Escarpments (black polygons denote escarpments investigated in this paper, white polygons denote escarpments mentioned in this paper).

1.4. Objectives of This Study

In this study we combine morphological observations from multibeam echosounder data with 3-D numerical modeling to:

(i) Determine if and how groundwater seepage can drive the formation of box canyons in submarine carbonate escarpments;
(ii) Assess the relative importance of box canyon formation as an erosional process across a carbonate escarpment.

The study focuses on the Florida Escarpment to address objective (i), and it also takes into consideration the Blake, Campeche and Malta Escarpments to fulfill objective (ii) (Figure 1). We have chosen these escarpments because they are amongst the best mapped and investigated globally. The Florida Escarpment, in particular, has been the most intensively studied and is the only escarpment where fluid seepage has been documented thus far.

1.5. Motivation

An improved understanding of carbonate escarpment evolution is of interest from both an academic and an applied standpoint. First, exposed submarine carbonate escarpments provide modern analogs of their buried counterparts. Carbonate escarpments are common in the geological record, with buried Mesozoic carbonate platform edges rimming much of the North Atlantic and passive continental margins along the Tethyan Seaway during the Mesozoic (Arthur et al., 1979; Given, 1977; Goldflam et al., 1980; Lancelot & Seibold, 1977; Locker & Buffler, 1983; Ryan & Miller, 1981; Schlee et al., 1979). Second, carbonate escarpments are commonly eroded by submarine canyons and landslides. The dynamics and controls associated with these processes are poorly constrained because most studies have focused on siliciclastic margins. As a result, our ability to estimate the hazards from these submarine processes to coastal communities and seafloor infrastructures is still poor. Third, carbonate platforms, slopes, and syn-stratigraphic units can host petroleum or ore bodies due to their high porosity and permeability. Knowledge on the geometry of these formations in the sub-surface and their controls is valuable to resource prospecting.

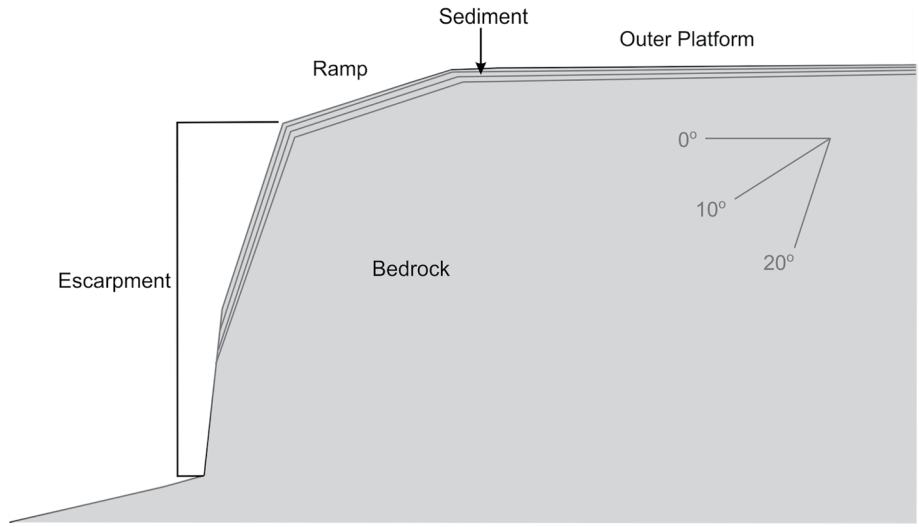

Figure 2. Cross-section through a carbonate margin illustrating the defined elements.

1.6. Definitions

In this paper the following definitions are used (Figure 2). A carbonate platform is an extensive submarine, gently sloping plateau constructed primarily by biological precipitation of calcium carbonate. Here reference is only made to the morphology and composition, and there is no differentiation between carbonate factories (sensu Schlager, 2005) or based on whether the platform is active or drowned. The ramp is an area of increased slope gradient in the outer part of the carbonate platform, where the gradient is <5° (Mullins et al., 1988). A carbonate escarpment is steep seafloor (>5°) with exposed bedrock, in places covered by a thin sediment cover, located between the outer platform or ramp and the abyssal plain.

2. Geological Framework

2.1. Florida Escarpment

The Florida Escarpment is ~640 km long and 1,600 m high, with a maximum local slope gradient of 74°. It marks the western boundary between the Florida-Bahama platform and ramp, and the deep waters of the Gulf of Mexico. The contact between the base of the escarpment and the abyssal plain of the Gulf of Mexico deepens from 2,600 to 3,400 m from north to south and has been buried by rapidly accumulating distal Mississippi Fan sediments (Paull et al., 1984; Twichell et al., 1990). Rocks exposed across the Florida Escarpment include bedded Early to Late Cretaceous, platform-interior lagoonal skeletal limestones and crystalline dolomite (Carannante et al., 1988; Corso et al., 1989; Freeman-Lynde, 1983; Paull, Freeman-Lynde, et al., 1990; Paull, Spiess, et al., 1990; Paull, Twichell, et al., 1991). Dredged and submersible samples show a change in age from Lower Aptian at the base of the escarpment to Upper Cenomanian at a depth of 1,950–2,200 m (Freeman-Lynde, 1983; Paull, Freeman-Lynde, et al., 1990). Above a depth of 1,500 m are gently sloping ramps covered by pelagic sediments deposited during the Tertiary (Carannante et al., 1988). Normal faults occur throughout the Lower Cretaceous and Jurassic sections (Corso et al., 1989; Shaub, 1984). They are concentrated in the Tampa and South Florida Basins, and may be due to basin subsidence and/or the collision of Cuba with the Florida-Bahama platform in the Early Cenozoic (Klitgord & Schouten, 1986; Twichell et al., 1990). There is little indication of faulting across the Tertiary to recent section (Corso et al., 1989; Shaub, 1984). Joints are oriented parallel and perpendicular to the escarpment face; they may be a relatively surficial characteristic in response to spalling or, more likely, reflect a regional fabric. The latter is generated by either the interaction of the Caribbean and North American plates during the Late Cretaceous and Tertiary (Klitgord & Schouten, 1986; Uchupi & Emery, 1968), or by differential subsidence across the basement features (Klitgord et al., 1984).

Active chemosynthetic biological communities, commonly referred to as cold seeps, were first discovered at the base of the Florida Escarpment, along with unique sedimentary deposits that contain anomalous amounts of authigenic sulphide minerals, carbonate cements and mussel shell hash (Chanton et al., 1991; Commeau et al., 1987; Hecker, 1985; Paull et al., 1984, 1992). Seepage is estimated to be occurring along ~10% of the base of the Florida Escarpment (Paull et al., 1988). The chemical and isotopic signatures of seep fluids suggest it consists of 6% platform formation brines and 94% seawater (Chanton et al., 1991, 1993; Martens et al., 1991; Paull et al., 1984). The brines consist of sulphide-rich fluids, due to dissolution of evaporite sulphate deposits within the platform, which are also rich in ammonium, methane, chloride and alkaline earth elements. Fluid circulation within the Florida-Bahama platform is density-driven and occurs at depths of >1 km. Seawater enters the carbonate platform along its exposed flanks below an impermeable anhydrite formation, percolates downwards through the platform, and seeps at the base after encountering an impermeable sill of hemipelagic sediments (Chanton et al., 1991; Fanning et al., 1981; Hughes et al., 2007; Kohout, 1965; Manheim & Horn, 1968; Paull & Neumann, 1987). Mixing between the brines and the seawater at the seepage sites is thought to give rise to corrosion as a result of mixing of waters of different salinities and the generation of acidic fluid due to seafloor oxidation of dissolved sulphide species (Chanton et al., 1991; Hanshaw & Back, 1980; Paull & Neumann, 1987; Paull, Spiess, et al., 1990; Plummer, 1975; Twichell et al., 1991). The effect of active corrosion has been observed in the form of pitted and fluted stratal surfaces, joint planes that are opened and enlarged, absence of Fe-Mn oxide coating and fine sediment drape where seepage occurs, and etched calcareous nannofossils in seep sediments at the base of the escarpment (Chanton et al., 1993; Paull & Neumann, 1987). Seepage and corrosion have also been inferred along terraces above the Florida Escarpment base, which mark the location of permeability horizons within the platform and suggest that seepage may occur at different depths (Paull et al., 1988; Twichell et al., 1991). Seeps are also associated with downslope, density-driven flows of briny fluids, generating fan-shaped deposits on the abyssal plain (Paull et al., 1992).

2.2. Blake, Campeche and Malta Escarpments

The characteristics of the Blake, Campeche and Malta Escarpments are summarized in Table 1. Their description is less detailed than for the Florida Escarpment because our modeling is only carried out for the latter (Section 3.2). Total escarpment lengths vary between 290 km (Malta Escarpment) and 810 km (Campeche Escarpment). Blake Escarpment is the highest (3,300 m) and steepest (83°) of the four escarpments. All three escarpments consistently correspond to sections composed of Mesozoic strata. The base of the escarpments comprises a sharp concave change in slope and a linear plan shape. Above the escarpments, the ramps are predominantly concave in profile and their downslope limit consists of a sharp to gentle convex change in slope. The ramps of the Campeche and Malta Escarpments, located above 2 km water depths, consist of Cenozoic age strata. In the case of the Blake Escarpment, the ramp comprises the broad and nearly flat Blake Plateau at water depths shallower than 1,500 m. The Campeche Escarpment has undergone geologically instantaneous margin collapse as a result of the Chicxulub meteorite impact, which generated erosive gravity flows that were the source of the Cretaceous-Tertiary boundary deposit in the Gulf of Mexico (Bralower et al., 1998; Denne et al., 2013; Paull et al., 2014). The Malta Escarpment, on the other hand, is thought to have been exposed down to a depth of 2 km and eroded during the Messinian salinity crisis (Micallef et al., 2019). Since the onset of plate convergence between Africa and Europe during the Late Cretaceous, the Malta Escarpment was transformed from a passive margin into a mega-hinge fault system with an additional sinistral strike-slip component (Argnani & Bonazzi, 2005; Gutscher et al., 2016; Reuther et al., 1993).

3. Materials and Methods

3.1. Multibeam Echosounder Data

High resolution multibeam echosounder surveys, conducted over the last 30 years, were used in this study (Figure 3):

1. Blake Escarpment: acquired during cruises between 1984 and 2005 using Kongsberg EM-121 and EM-1002, SeaBeam, Seabeam 2112 and Atlas Hydrosweep systems;

Table 1
Morphological Parameters, Location and Exposed Lithologies for the Blake, Campeche and Malta Escarpments

Escarpment	Total length (km)	Maximum total vertical relief (m)	Maximum average gradient (°)	Maximum local gradient (°)[a]	Location	Exposed lithologies	References
Blake	350 (250 km covered by multibeam surveys)	3,300	27	83	Separates the eastern edge of the Blake Plateau from the deep waters within the Blake-Bahama Basin	Limestones and dolomites with facies indicating deposition in the shallow, quiet interior of a carbonate bank. Oldest rocks sampled have a Barremian and Hauterivian-Valanginian age.	Benson et al. (1978), Dillon et al. (1979, 1985, 1987)
Campeche	810	1,500	32	82	Northern edge of the Yucatan continental margin	Oligocene to Early Paleocene nannofossil ooze and chalk deposited in open marine conditions overlying an abrupt transition to Lower Cretaceous dolomites. The base of the Campeche Escarpment has been buried by distal Mississippi Fan sediments throughout the Cenozoic, at rates that reached maximum values of 6–11 m per 1 ka.	Bird et al. (2005), Feeley et al. (1985), Kohl (1985), Locker and Buffler (1983), Paull et al. (2014), Worzel et al. (1973)
Malta	290 (120 km covered by multibeam surveys)	1,100	35	74	Marks the boundary between the Pelagian Platform and the deep Ionian Basin	Late Triassic to Late Cretaceous shallow platform carbonates and Miocene shelf edge carbonate build ups. The entire Jurassic-Cretaceous succession is punctuated by tuffs and pillow lavas. Tortonian pelagic sediments cover the upper Malta Escarpment. The foot of the escarpment is buried underneath Jurassic to Quaternary sediments of the Ionian Basin.	Argnani and Bonazzi (2005), Biju-Duval et al. (1982), Bosellini (2002), Casero et al. (1984), Cernobori et al. (1996), Cita et al. (1980), Finetti (1982), Micallef et al. (2016, 2019), Nicolich et al. (2000), Pedley et al. (1993), Scandone et al. (1981), Speranza et al. (2012)

[a]Maximum local gradient is the maximum value of mean slope measured across circular zones with a diameter of 500 m covering the entire escarpment.

2. Florida Escarpment: acquired during cruises between 1988 and 2014 using Kongsberg EM-120, EM-710 and EM-302, SeaBeam, SeaBeam 2112 and Atlas Hydrosweep systems;
3. Campeche Escarpment: acquired during *R/V Falkor* cruise FK-007 in 2013 using Kongsberg EM-710 and EM-302 systems (Paull et al., 2014);
4. Malta Escarpment: acquired during cruises between 2012 and 2014 using Kongsberg EM-710 and EM-302 and Reson SeaBat 7150 and 8111 systems (Micallef et al., 2016, 2019).

Bathymetric data were gridded at 100 m to allow a uniform, quantitative comparison of escarpment morphology. Geomorphometric techniques were then utilized to map the boundaries and thalwegs of submarine canyons, as done in Micallef, Mountjoy, et al. (2014) and Micallef, Ribó, et al. (2014). These techniques included hydrology tools available in Geographic Information Systems, which involve the computation of flow direction and flow accumulation routines.

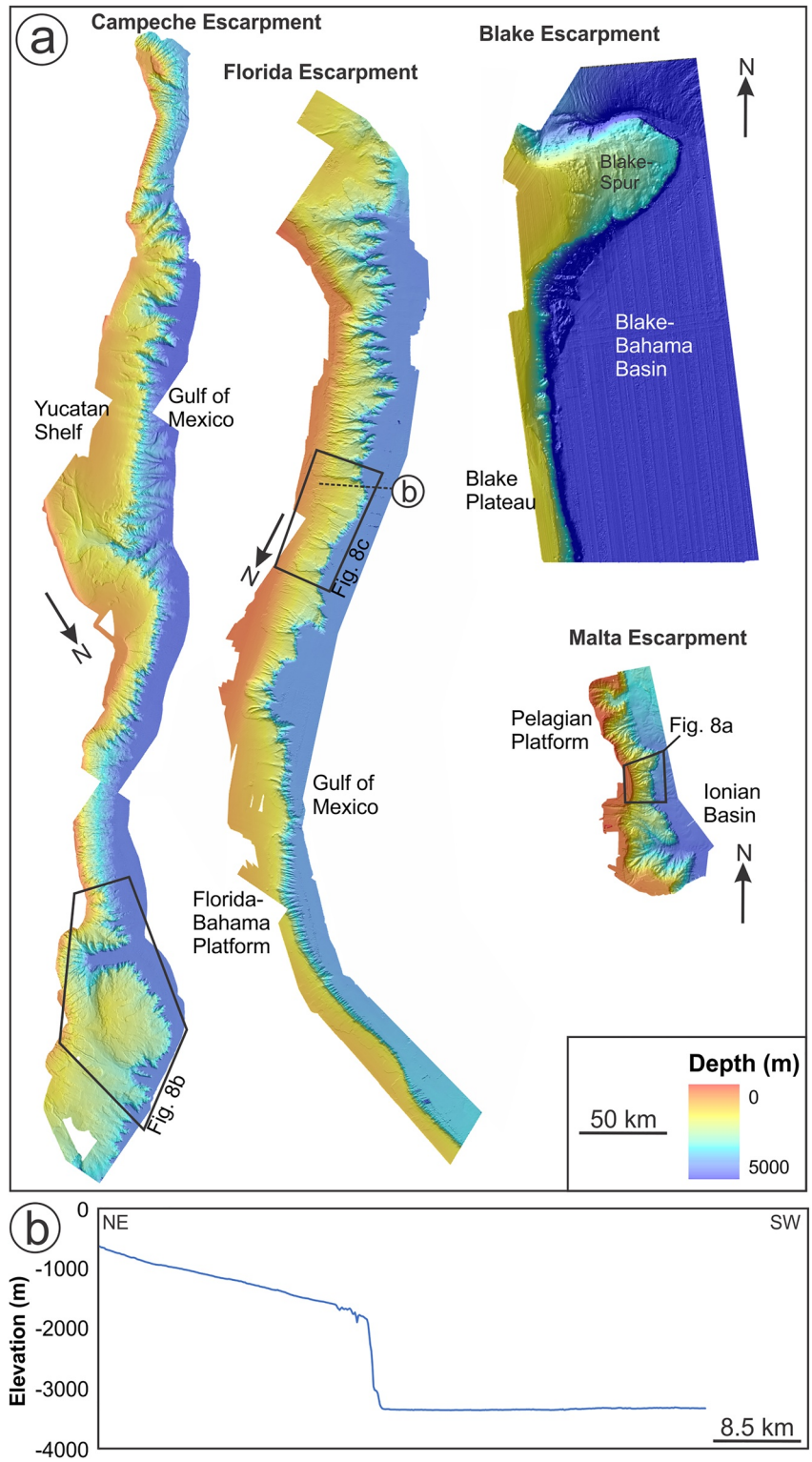

Figure 3. (a) Multibeam bathymetric maps of the Blake, Campeche, Florida and Malta Escarpments displayed at the same scale. (b) Cross-sectional profile across the Florida Escarpment. Location in (a).

3.2. 3-D Distinct Element Modeling

The commercially available software 3DEC (https://www.itascacg.com/software/3dec) was used to address the question of whether fluid seepage via joints can lead to their widening by fluid pressure (pore and joint fluid pressure) and dissolution, reduce the rock strength, and ultimately result in slope failure and the upslope evolution of a box canyon. A 3-D Distinct Element Model consists of discrete blocks represented as polyhedrons with planar boundaries that correspond to joints in a rock mass. The blocks are allowed to deform and they are internally discretized into finite-difference tetrahedral elements (Cundall & Strack, 1979). Displacements along joints, as well as rotations and collapse of blocks, are allowed. Fluid propagates through the model primarily through joints, and equations of motion are solved using an explicit solution scheme. 3DEC uses a finite volume formulation for calculating stress, strain and displacement.

3.2.1. Governing Equations

3.2.1.1. Joint Fluid Flow

As a first approximation, the fluid flow along a joint is modeled as flow between two parallel plates with constant hydraulic aperture (b_h), as described by the "cubic law" (Snow, 1965):

$$q = \frac{b_h^3 w \rho g}{12\mu} \Delta H \tag{1}$$

where q is the flow rate per unit width (w), ρ is the fluid density, g is the gravitational acceleration, μ is the fluid dynamic viscosity, and ΔH is the hydraulic head gradient.

The transient fluid flow in a joint with uniform hydraulic aperture is modeled using the diffusivity equation written in terms of the hydraulic head (H):

$$\frac{\partial H}{\partial t} = D\nabla^2 H \tag{2}$$

where ∇^2 is the Laplacian, t is the time, and D is the scalar hydraulic diffusivity (Hummel & Müller, 2009), which is defined by:

$$D = \frac{K}{S_i} = \frac{T}{S} \tag{3}$$

where S_i is intrinsic storativity, S is the increase in the weight of fluid stored per unit area of a joint, K is hydraulic conductivity, and T is the rate at which groundwater flows horizontally (transmissivity) (Cappa et al., 2008; Domenico & Schwartz, 1997). The latter is defined according to the parallel plate flow concept as:

$$T = \frac{\rho g w}{12\mu}\left[b_{hi} + \frac{\sigma_{ni}^{'}}{k_{nif}^{1/3}}\left(1 - \frac{\sigma_{ni}^{'}}{\sigma_n^{'}}\right)\right]^3 \tag{4}$$

where k_{nif} is the initial joint normal stiffness, σ_{ni} is the initial effective normal stress, b_{hi} is the initial hydraulic aperture at the initial effective stress, and $\sigma_n^{'}$ is the initial effective normal stress.

3.2.1.2. Elastic Hydromechanical Behavior of Joints

The relationship between effective normal stress ($\sigma_n^{'}$), normal stress (σ_n) and fluid pressure (P_f) is described by the effective stress law (Biot, 1941; Terzaghi, 1923):

$$\sigma_n^{'} = \sigma_n - \alpha P_f \tag{5}$$

where α is the Biot effective stress constant.

$$\sigma_n^{'} = \sigma_n - \left(1 - S_c\right)P_f \tag{6}$$

where S_c is the ratio of the contact area to total joint surface.

The storativity (S_e) expresses the increase in the weight of fluid stored per unit area of a joint in response to a unit increase in pressure, and can be defined according to Domenico and Schwartz (1997) as:

$$S_e = \frac{1}{A}\frac{\partial\left(\rho g V_f\right)}{\partial P_f} \tag{7}$$

where A is the area of the joint plane and V_f is the fluid volume between the two joint faces.

Under normal stress, the coupling between joint flow and normal deformation is modeled according to the "modified cubic law" (Witherspoon et al., 1980):

$$q = \frac{\left(b_{hi} + f\Delta U_n\right)^3 w\rho g}{12\mu}\Delta H \tag{8}$$

$$b_h = b_{hi} + f\Delta U_n \tag{9}$$

where b_{hi} is the initial hydraulic aperture at the initial effective stress and f is a factor reflecting the influence of roughness on the tortuosity of flow. This law associates the joint hydraulic aperture (b_h) to the joint normal displacement (U_n).

Joint displacements are induced by a change in the effective stress field acting on the joint. The relationship between stresses and joint displacement is described by the relation between the change in joint normal and shear displacements (respectively, noted U_n and U_s) caused by a change in effective normal ($\sigma_n^{'}$) and shear ($\sigma_s^{'}$) stresses (Goodman, 1970):

$$\Delta U_n = \frac{\Delta\sigma_n^{'}}{k_n} \tag{10}$$

$$\Delta U_s = \frac{\Delta\sigma_s}{k_s} \tag{11}$$

where k_n and k_s are the normal and shear stiffness, respectively.

3.2.1.3. Joint Dissolution

Joint dissolution cannot be explicitly modeled with a Distinct Element Model. This process was therefore simulated by assuming that the change in joint volume with time ($\Delta V(t)$) is equivalent to the volume of dissolved mineral (Vm), which was calculated as follows (adapted from Garcia-Rios et al., 2015):

$$Vm\left(t\right) = kQ\int_{t'=0}^{t'=t} dt' \tag{12}$$

where Q is the flow rate and k is a constant.

3.2.2. Model Parameters for Florida Escarpment

A 3-D Distinct Element Model was developed for a section of the Florida Escarpment. The initial model geometry consists of a flat shelf, a linear escarpment and a flat abyssal plain (Figure 4). The domain's dimensions are 1,000 m (length) by 1,000 m (width) by 200 m (height). The geotechnical properties used in the model (Table 2) are for dolomite and derived from borehole data, seafloor imagery and geophysical surveys from onshore/offshore Florida and elsewhere. Groundwater, driven by a hydraulic head, is supplied from the landward side of the carbonate platform, and the direction of groundwater flow is from the escarpment into the ocean. The base of the model is considered impermeable. The initial pore water pressure within the escarpment was estimated by accounting for a 500 m high seawater column above the top of escarpment, and was added to all nodes of the model. This value was chosen because the boundary between the ramp and outer platform above the Florida Escarpment is located at a water depth of ~500 m.

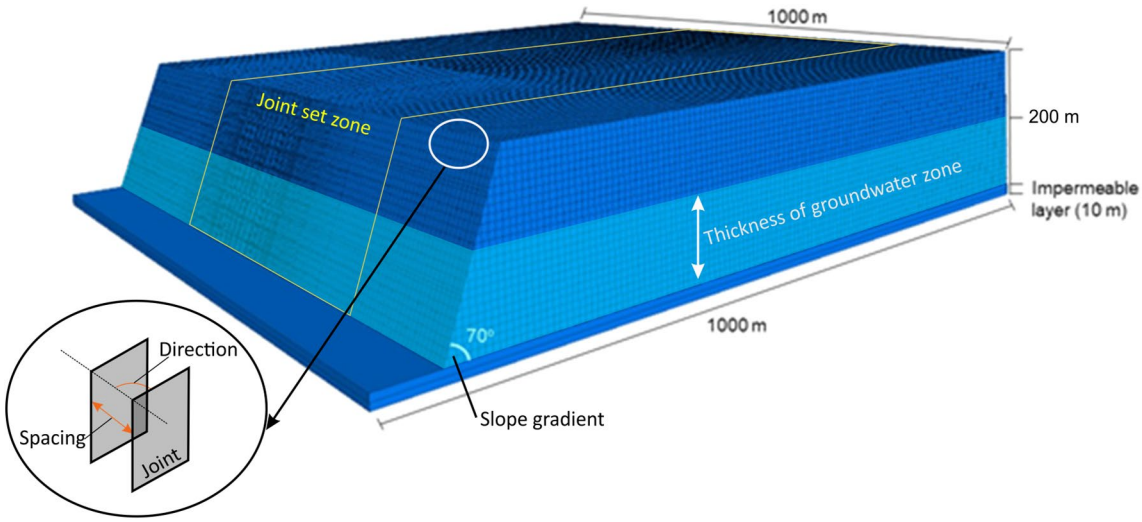

Figure 4. Geometry of the 3-D Distinct Element Model domain.

For the main model, the following parameters were used: (a) a constant slope gradient of 70° for the escarpment; (b) a 100 m thick flowing groundwater zone at the base (i.e., half the vertical extent of the domain); (c) two basic (intrinsic) joint sets with a uniform density of 0.2 per m with orientations perpendicular and parallel to the escarpment (Figure 4; Table 2). A third joint set, assumed to result from external processes (e.g., faulting, tectonics), was imposed across the joint set zone, which is a central 500 m wide section of the escarpment (Figure 4). This joint set is oriented perpendicular to the escarpment and entails an exponential decrease in joint density from 2 per m at the center to 0.2 per m at the boundaries (i.e., correlation between joint density and distance is exponential). Such a spatial variation in joint density is representative of field observations of fracture distribution across fault zones (e.g., Caine et al., 1996; Liao et al., 2019; Sagy et al., 2001; Wilson et al., 2003).

In addition, a number of additional simulations were carried out by individually changing the following parameters to test their influence on the shape, size and evolution of box canyons:

1. A linear decrease in joint density across the joint set zone from a maximum of 2 per m at the center to a maximum of 0.2 per m at the boundaries;
2. A uniform joint density of 0.4 per m across the joint set zone;
3. Thickness of the flowing groundwater zone above the base of 25 m;
4. Basic joint density divided by 5;

Table 2
Geotechnical Properties for Dolomite Used in the 3-D Distinct Element Model

Property	Units	Value	References
Young's modulus	GPa	37.8	McVay et al. (2019), Yasar and Erdogan (2004)
Poisson's ratio	-	0.28	McVay et al. (2019), Palchik (2019)
Bulk density	kN/m^3	29.5	Koumantakis and Sachpazis (1989), Yasar and Erdogan (2004)
Joint direction	°	0, 90	Paull, Spiess, et al. (1990)
Joint density	m^{-1}	0.2	Paull, Spiess, et al. (1990)
Friction angle	°	48	Nguyen (2020)
Joint normal stiffness	MPa	1.7	Nguyen (2020)
Joint shear stiffness	MPa	2.1	Bandis et al. (1983), Rodgers et al. (2018)
Porosity	%	1.2	Koumantakis and Sachpazis (1989), Maricic et al. (2018)
Hydraulic conductivity	m/s	10^{-6}	Domenico and Schwartz (1997), Heath (1985)

5. Basic joint direction rotated by 45° clockwise;
6. Escarpment slope gradient of 45°.

3.2.3. Simulations

Each model simulation entailed a total of 4 million calculation cycles. Each cycle is composed of a sequence of operations based on one year of groundwater flow. The boundary conditions evolved as the model domain changed due to removal of blocks. In our model, the rock blocks disappeared once they became detached from the cliff face. In addition, the enhancement of dissolution at the seepage sites due to the mixture of waters with different salinities was ignored.

4. Results

4.1. Morphology

Canyons and scars are the most common landforms in all four carbonate escarpments.

4.1.1. Canyons

Two very distinct groups of canyon morphologies can be identified (Figures 5–9):

1. V-shaped canyons, which have high length:width ratios (>2) and drainage densities (>0.3 km^{-1}), low mean spacing (<4 km) and bifurcation angles (<40°), V-shaped cross-sections, gentle to steep wall gradients (<25°), sharp interfluves, pointed heads and concave thalweg profiles.
2. Box canyons, which have low length:width ratios (<2) and drainage densities (<0.3 km^{-1}), high mean spacing (>4 km) and bifurcation angles (>40°), U-shaped cross-sections, steep to vertical wall gradients (>25°), theater-shaped heads and linear thalweg profiles.

Overall, v-shaped canyons are consistently more prevalent (Table 3); they are located either on the ramp or gently sloping (<10°), concave sections of the escarpment. In the Campeche and Malta Escarpments, they tend to be located where the 120 m isobath (Last Glacial Maximum palaeo-coastline) is closest to the escarpment top. Box canyons are only found at the base of escarpments. The Florida Escarpment has the largest number of canyons (n = 301). Box canyons are concentrated in two areas—between 24°20′N and 25°35′N, and between 26°30′N and 27°N. The largest canyon on the Florida Escarpment is the Florida Canyon, which is a 20 km long and 4 km wide box canyon (Paull, Spiess, et al., 1990). The ratio of area per length is higher for box canyons than for v-shaped canyons in the Campeche, Florida and Malta Escarpments, and vice-versa for the Blake Escarpment (Table 3). The Campeche Escarpment has the highest area of box canyons, both total and per escarpment length (Table 3), of any escarpment, and it also hosts the largest box canyon, which is 24 km long and 7.6 km wide.

4.1.2. Scars

Scars are downslope-oriented depressions with low aspect ratios. The headwalls of the scars are generally steep (10–25°) and linear to arcuate in plan shape. At their distal limit, most scars connect to either another scar or a canyon. The seabed within these scars is typically relatively smooth and planar. Scars are predominantly located on the ramps (Table 3), where they have a mean area of ~10 km^2 and headwall heights of 100–200 m. The largest scar has an area of 480 km^2 (in the Campeche Escarpment). The smallest scars are located along the heads and walls of submarine canyons. The Florida Escarpment has the largest area of scars per escarpment length, although the largest area of scars across the escarpment face is observed at the Campeche Escarpment (Table 3).

4.2. Numerical Simulations

The results of all numerical simulations are presented as four consecutive snapshots of a duration of 1 million cycles (Figure 10). For the main model, a box canyon—with a theater-shaped head, linear thalweg profile, steep to vertical wall gradients, and a length of 423 m—develops by the end of the simulation (Figure 10). The initial stages involve the development of a recess and an overhang along the base of the escarpment. This eventually leads to loss of support and failure of the cliff face via toppling and rock fall.

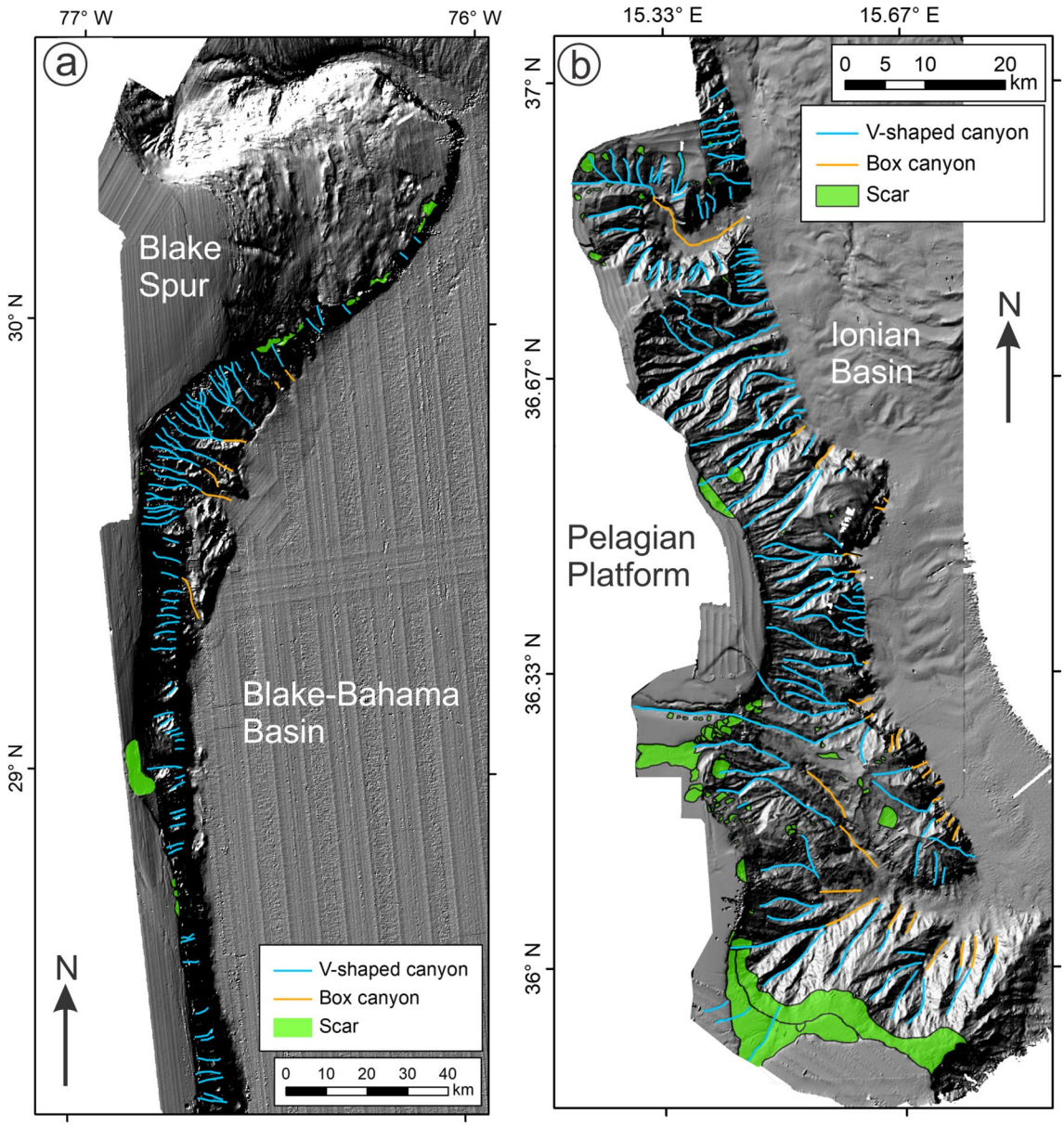

Figure 5. Shaded relief maps of (a) Blake Escarpment and (b) Malta Escarpment with interpreted landforms superimposed.

Recurrence of these mechanisms results in the landward retreat of the canyon head; this retreat is faster at the center and slower at the sides due to the lateral variability in joint density across the joint set zone.

The results from the additional simulations using different parameters are summarized in Table 4.

5. Discussion

5.1. Origin of V-Shaped Canyons and Scars

In siliciclastic margins, gravity flows are known to incise submarine canyons characterized by v-shaped cross-sectional shapes, concave thalweg profiles and dendritic network patterns (Gerber et al., 2009; Mitchell, 2005; Pratson et al., 2009). In view of the similarity with such morphologies, v-shaped canyons in carbonate escarpments have been associated with pelagic and hemipelagic sediments traveling as channelized debris flows and turbidity currents, collectively referred to here as gravity flows. The latter are thought to

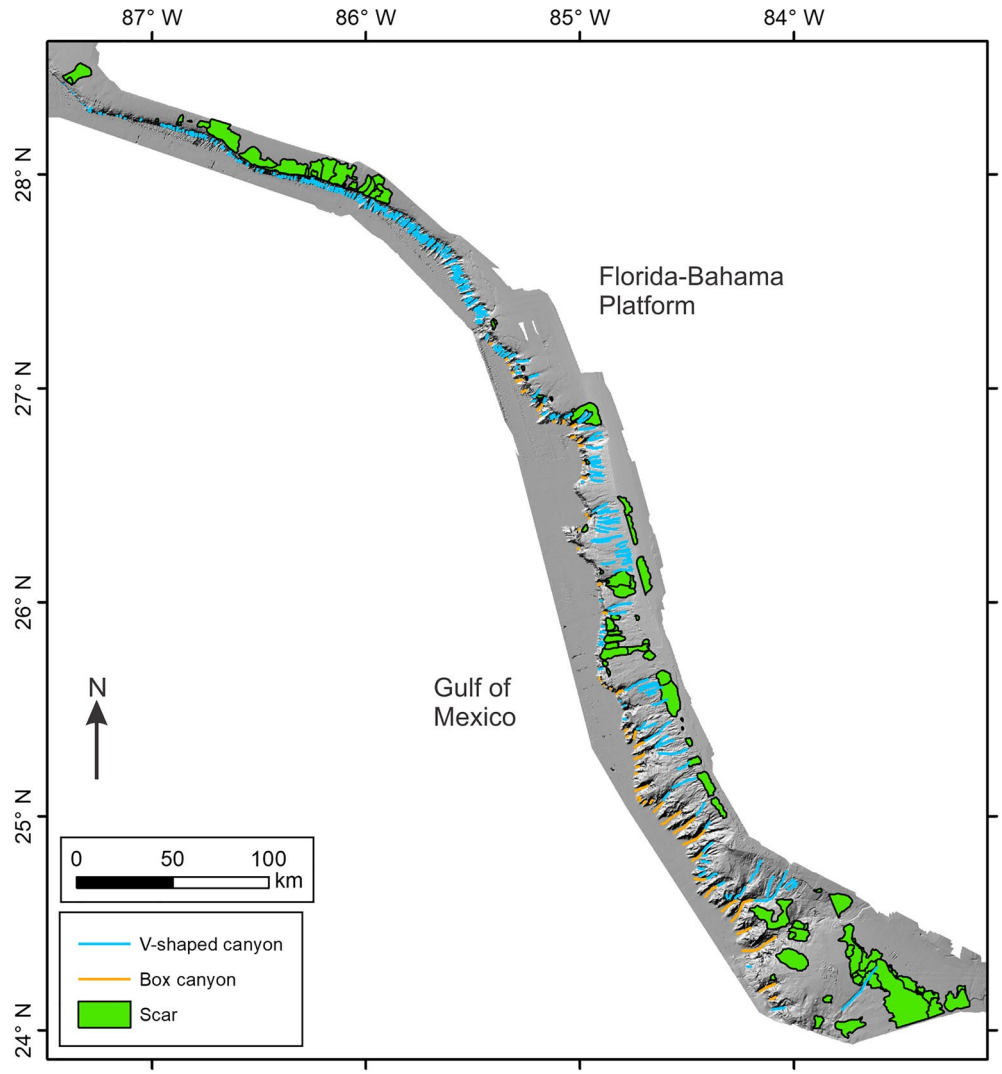

Figure 6. Shaded relief map of Florida Escarpment with interpreted landforms superimposed.

mechanically erode the v-shaped canyons and form debrites, turbidites and extensive carbonate lenses at the foot of the escarpment (Casero et al., 1984; Holmes, 1985; Lindsay et al., 1975; Micallef et al., 2019; Paull, Freeman-Lynde, et al., 1990; Paull, Spiess, et al., et al., 1990; Twichell et al., 1996). Most gravity flows are sourced by terrestrial sediments during sea-level lowering (e.g., subaerial fluvial discharge, hyperpycnal flows), failure of pelagic and hemipelagic sediments, or strong surface current flowing across platforms (Casero et al., 1984; Lindsay et al., 1975; Micallef et al., 2019; Wilson & Roberts, 1992). The former is supported by the spatial correlation of v-shaped canyons on escarpments with sea-level lowstand coastlines in the Campeche and Malta Escarpments.

On escarpments, erosion by gravity flows is thought to be restricted to the sediment veneer (Bryant et al., 1969; Freeman-Lynde, 1983; Paull, Freeman-Lynde, et al., 1990; Twichell et al., 1996). However, we do see a stark difference in the morphology of the escarpments—gentler slope gradient, convex slope profile—where the v-shaped canyons are located. This suggests that the Mesozoic carbonate bedrock has been eroded, and this may be attributed to quarrying and plucking by the gravity flows, which is particularly effective in jointed bedrock (Mitchell, 2014).

Scars are the result of submarine mass movements triggered by loss of support and steepening associated to erosion downslope (Micallef et al., 2019; Mullins & Hine, 1989; Twichell et al., 1990, 1996). The larger, more prevalent scars are the result of failure in sedimentary drape across the ramp.

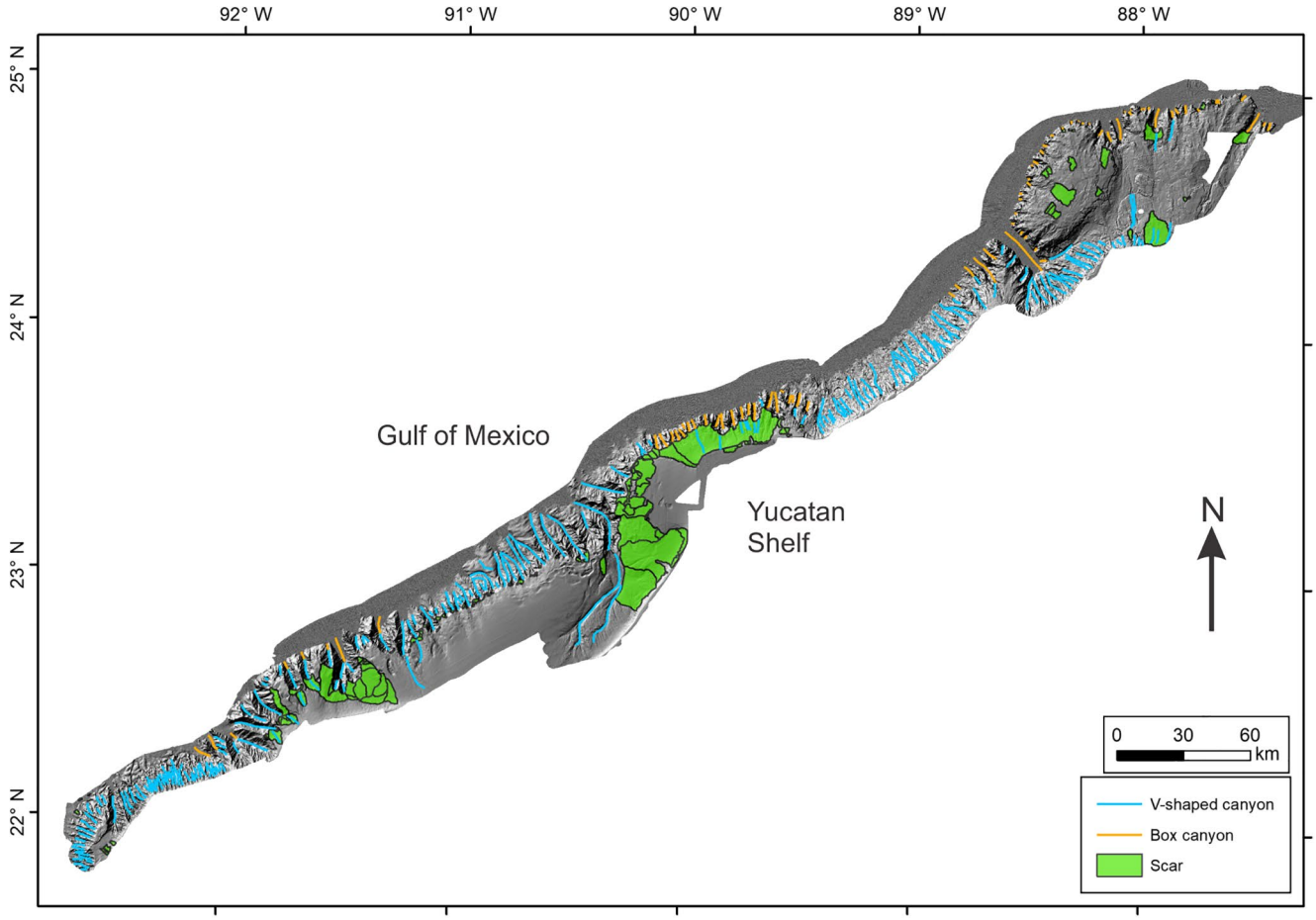

Figure 7. Shaded relief map of Campeche Escarpment with interpreted landforms superimposed.

The morphological differences between carbonate escarpments, in terms of v-shaped canyons and scars, can be attributed to the following:

1. High sedimentation rates (up to 6–11 m per 1 ka, as estimated from scientific drilling samples) during the Cenozoic (Kohl, 1985) may explain why the upper Campeche and Florida Escarpments host the largest landslides and have the highest scar area per escarpment length on their ramps.
2. Blake Escarpment features the lowest frequency of canyons and scars, which may be attributed to low sedimentation supply since the Palaeocene/Eocene due to the presence of the Florida Current (Gulf Stream). The latter eroded young sediments, prevented terrigenous sediment input to the Blake Plateau and reduced erosive mass wasting downslope (Dillon & Popenoe, 1988; Dillon et al., 1985; Popenoe, 1985; Sheridan, 1981).
3. The highest percentage of v-shaped canyons is observed across the ramp of the Malta Escarpment, and this is likely due to subaerial exposure and fluvial incision during the Messinian salinity crisis (Micallef et al., 2019).

5.2. Formation of Box Canyons by Fluid Seepage at the Florida Escarpment

The results of our numerical simulations confirm that fluid seeping via joints can lead to the retrogressive evolution of a box canyon at the base of the Florida Escarpment via episodic block failure at the head due to a reduction in rock strength (Figures 10 and 11). A box canyon formed at the end of all simulations, even when the model parameters were changed (Figure 10). According to Table 4, the box canyon tends to be longer when:

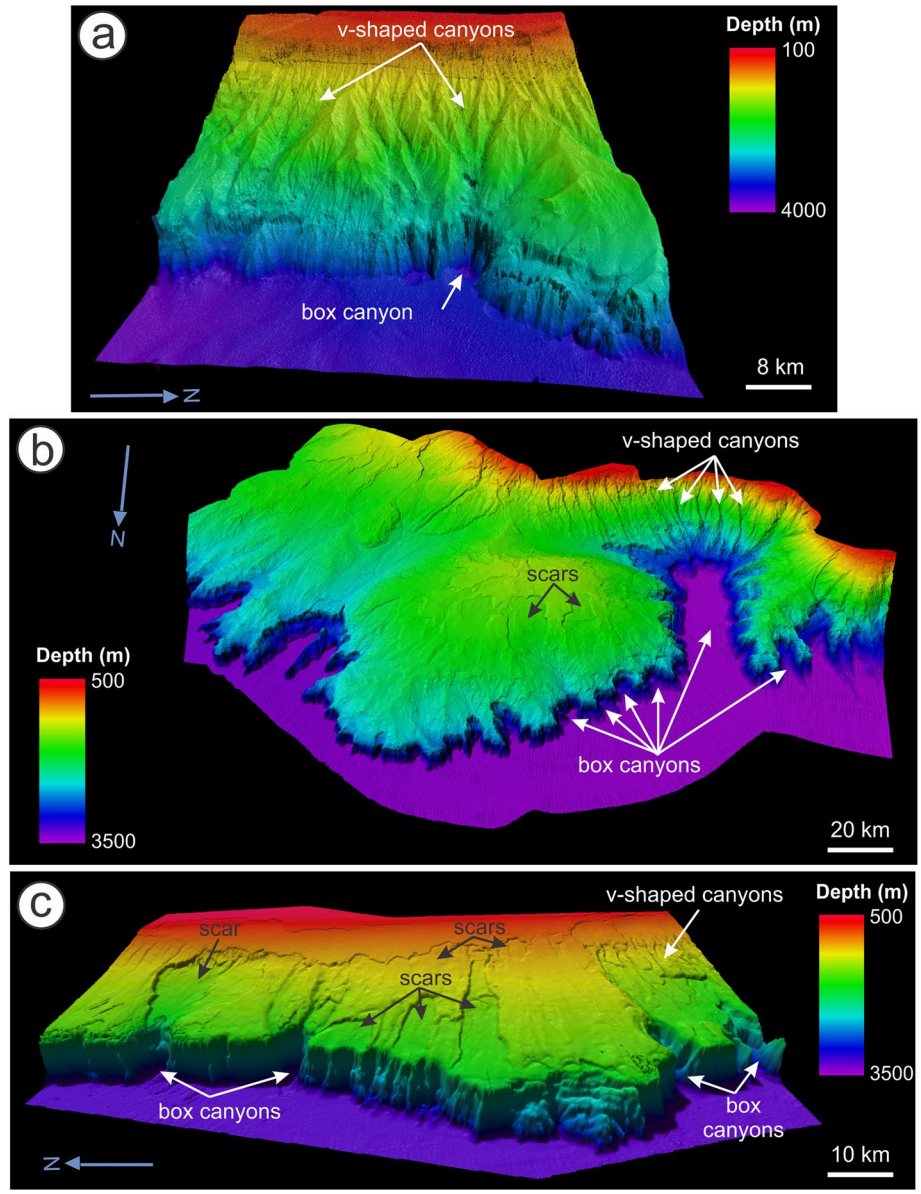

Figure 8. 3D renderings of bathymetry illustrating v-shaped canyons, box canyons, and scars on the (a) Malta Escarpment, (b) Campeche Escarpment and (c) Florida Escarpment. Location in Figure 3.

1. The basic joints are oriented perpendicular and parallel to the escarpment (joints are subjected to the highest normal stresses when they are oriented at or near to perpendicular to the loading direction [Jaeger et al., 2007; Singh et al., 2002]);
2. The basic joint density is higher (a higher joint density results in smaller blocks that are easier to mobilize);
3. The distribution of joint density across the joint set zone is exponential (such a distribution is associated with the highest overall joint density across the joint set zone);
4. The thickness of the flowing groundwater zone is higher (fluid pressure and dissolution affect a larger extent of the escarpment);
5. The slope gradient of the escarpment is higher (slope failure is facilitated by steeper slopes).

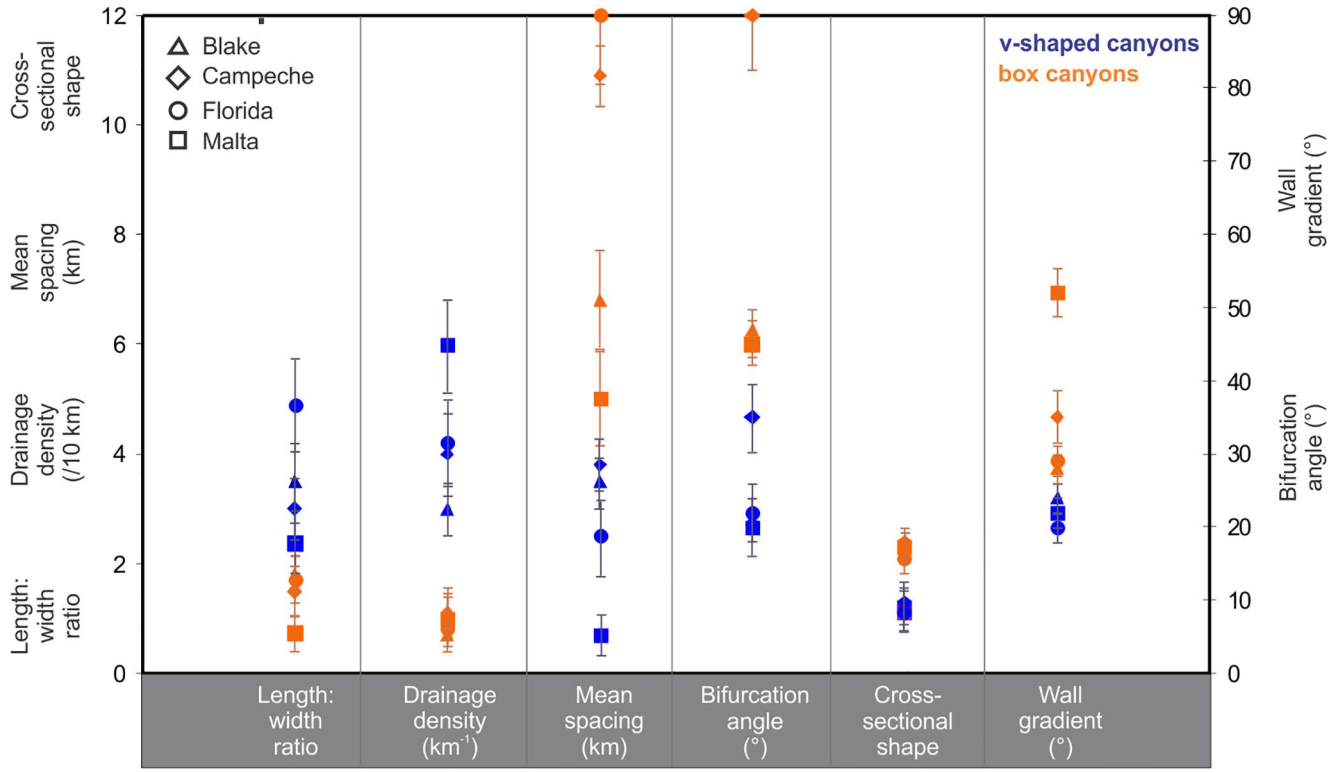

Figure 9. Plots of mean and standard deviation of morphologic parameters for v-shaped and box canyons for all carbonate escarpments. The parameters were measured as follows: (i) Length:width ratio—thalweg length divided by width. (ii) Drainage density—Total thalweg length of a canyon system (including tributaries) divided by area. (iii) Mean spacing—Linear distance between center points of two adjacent canyons. (iv) Bifurcation angle—angle at the bifurcation of a canyon into two tributaries. (v) Cross-sectional shape—Calculated by normalizing each side of a cross-sectional profile, reducing them into a power law curve, and using the exponent as a shape indicator (Brook et al., 2006). Exponent of ~1 represents a V-shaped canyon. The value 2 describes a U-shaped canyon, >2 denotes a wide flat valley bed and is typical of a box canyon. (vi) Wall gradient—Slope gradient of the steepest wall for an individual canyon. Number of canyons at each escarpment: Blake (90), Campeche (281), Florida (301), Malta (153).

The angularity of the canyon head tends to decrease when the joint density across the joint set zone is uniform or when the basic joint density is lower (Figure 10). In our simulations, the width of the box canyon is controlled by the width of the joint set zone.

The observations at the base of the Florida Escarpment are consistent with the model predictions. The occurrence of patches of talus composed of rectangular blocks on the canyon floors, indicative of periodic collapse, are more common at the base of the canyon heads (Paull, Twichell, et al., 1991). The growth rate of the box canyon in our main scenario is estimated at 10 km per 100 Ma, which compares well with the escarpment retreat of 8 km in the last 100 Ma inferred from geophysical data (Corso & Buffler, 1985; Freeman-Lynde, 1983; Paull, Freeman-Lynde, et al., 1990).

The occurrence of box canyons across the Florida Escarpment coincides with the location of basins (e.g., Tampa Basin, South Florida Basin) under the west Florida shelf, where faulting of the Cretaceous and Jurassic strata is concentrated (Ball et al., 1988; Twichell et al., 1990). The location of basins also coincides with more abundant anhydrite (Applin & Applin, 1965), which implies a larger source of dense, sulphide-rich brines discharging along the escarpment.

Based on the above, we conclude that there are three main factors supporting box canyon formation along the base of the Florida Escarpment: (a) an internal, density-driven fluid circulation system that leads to the seepage of corrosive fluids at the base of the escarpment (Chanton et al., 1991, 1993; Paull & Neumann, 1987; Paull et al., 1988), (b) limestone and dolomite outcrops that are susceptible to dissolution, and (c) fabric (joints, faults), which enhances groundwater flow to and seepage across the escarpment, and facilitates fragmentation and failure of massive rock faces.

Table 3
Number and Area[a] of Canyons and Scars and Across the Ramps and Escarpments

Canyons									
Escarpment	Canyons (#)	Canyons (V-shaped) (#)	Canyons (box) (#)	V-shaped canyon area across ramp (km^2)	V-shaped canyon area per length across ramp (km^2 km^{-1})	V-shaped canyon area across escarpment (km^2)	V-shaped canyon area per length across escarpment (km^2 km^{-1})	Box canyon area across escarpment (km^2)	Box canyon area per length across escarpment (km^2 km^{-1})
Blake	90	81 (90%)	7 (10%)	755	3.0	1,081	4.3	268	1.1
Campeche	281	205 (73%)	76 (27%)	900	1.1	5,863	7.2	5,888	7.3
Florida	301	249 (83%)	52 (17%)	2,492	3.9	1,053	1.6	1,521	2.4
Malta	153	123 (80%)	30 (20%)	1,000	8.3	428	3.6	644	5.4

Scars					
Escarpment	Scars (#)	Scar area across ramp (km^2)	Scar area per length across ramp (km^2 km^{-1})	Scar area across escarpment (km^2)	Scar area per length across escarpment (km^2 km^{-1})
Blake	14	90	0.4	0	0
Campeche	131	2,761	3.4	83	0.10
Florida	90	3,115	4.9	17	0.03
Malta	186	259	2.2	1	0.01

[a]Canyon area was estimated based on the boundaries of submarine canyons delineated semi-automatically using morphometric attribute maps (slope gradient, slope aspect, profile curvature), flow accumulation map and water basin analysis.

5.3. Significance of Box Canyon Formation in Escarpment Erosion

Across the Campeche, Florida and Malta Escarpments, box canyons are, in terms of areal extent, more prevalent than either v-shaped canyons or scars (Table 3). Box canyons also cover a greater proportion of the escarpment area than scars at the Blake Escarpment. Box canyon formation is, therefore, a significant erosive process across carbonate escarpments.

5.4. Implications

5.4.1. Implications for Other Carbonate Escarpments

Is the model for box canyon formation proposed for the Florida Escarpment (Figure 11) applicable to the Blake, Campeche and Malta Escarpments?

All three sites share lithological similarities with the Florida Escarpment, with outcrops of limestone and dolomite (Table 1), and with joints being similarly ubiquitous. Box canyons at the Blake Escarpment have been linked to jointing due to a regional fabric, uneven erosional unloading of the escarpment's face, or differential subsidence across the fracture zone (Dillon et al., 1987, 1993; Paull, Twichell, et al., 1991). Little is known of the fabric of the Campeche Escarpment, although offsets of up to 100 m have been observed in seismic reflection profiles, some of which are likely related to the Chicxulub impact structure (Gulick et al., 2013; Morgan et al., 1997). The Malta Escarpment exhibits both Mesozoic normal block faulting and a more recent sinistral strike-slip component (Catalano et al., 2000; Grasso, 1993; Gutscher et al., 2016; Pedley et al., 1993; Reuther, 1990; Reuther et al., 1993; Scandone et al., 1981), whilst vertical jointing is clearly visible in seafloor images (Biju-Duval et al., 1982).

Although fluid seepage has only been documented at the base of the Florida Escarpment, density-driven circulation cells may be active in other carbonate escarpments as well. At the Florida Escarpment, the occurrence of evaporites is the main reason for the development of an outward flow at the base of the escarpment. There are indications for the occurrence of evaporites in the other escarpments. Evaporites have been reported in onshore and offshore wells at depths of 1 and 5 km in the Malta Plateau (Bishop & Debono, 1996; Gatt, 2012). Extensive beds of gypsum/anhydrite-bearing evaporite of probable Palaeogene age outcrop across the Campeche Escarpment (Hudec & Norton, 2019; Perry et al., 2012). Porewater records

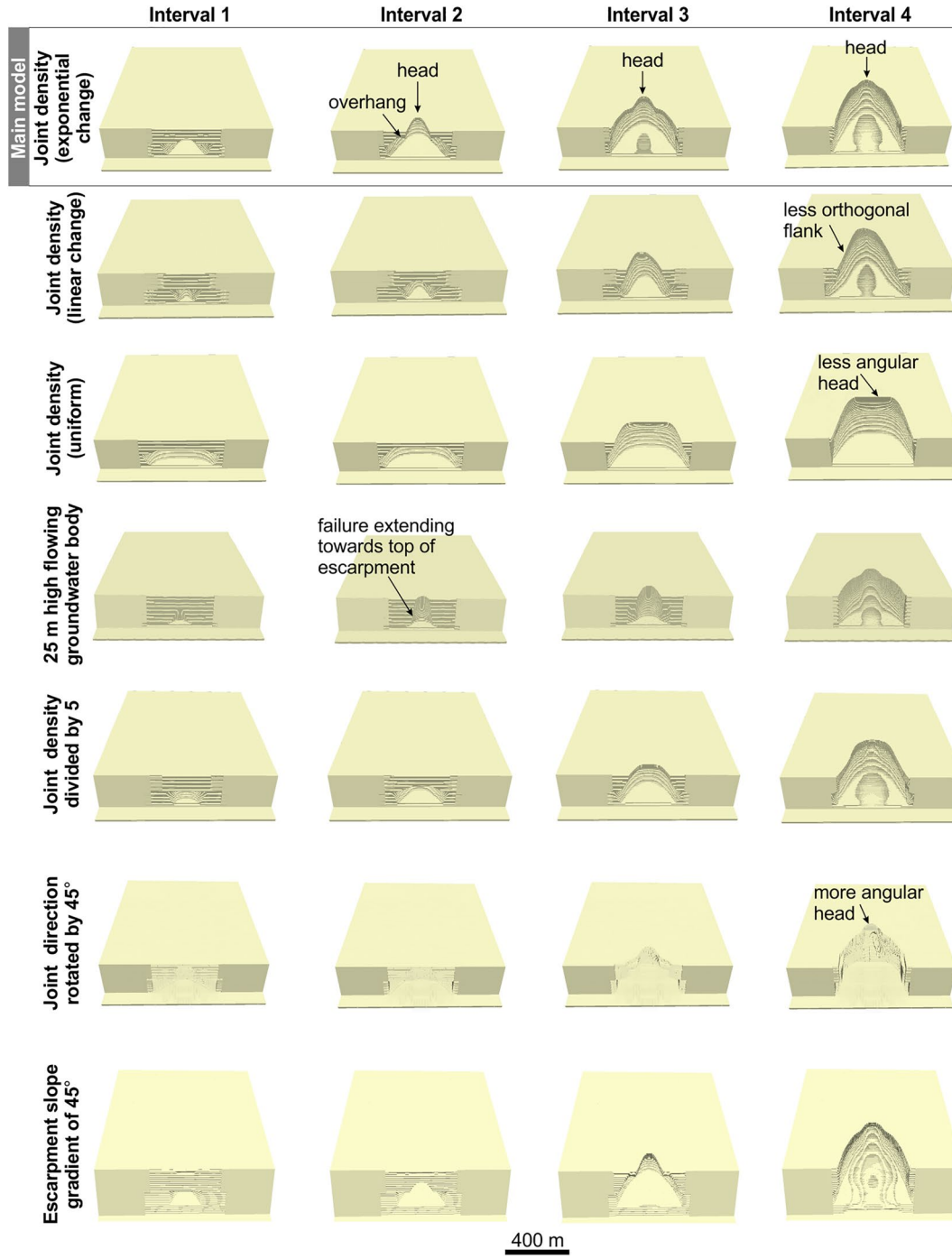

Figure 10. Evolution of box canyon morphology during four consecutive intervals, as simulated for the Florida Escarpment, for different parameters. Each interval is 1 million calculation cycles, which is equivalent to 1 Ma.

from ODP Site 1052, drilled in the Blake Escarpment, show significant increases in salinity, chloride, and sodium concentrations with depth, which may indicate the presence of an evaporite sequence in the underlying Cretaceous and Jurassic units (Norris et al., 1998). In addition, circulation cells within carbonate platforms can also be stimulated by lateral thermal differences and changes in sea level, among others (Hughes et al., 2007; Kohout, 1965; Manheim, 1967). Escarpments are also fundamental hydrological boundaries, with their base acting as a "triple point" between the abyssal seawater and the waters within the platform

Table 4
Description of Box Canyon Evolution and Length for the Different Parameters Simulated

Parameter	Description of box canyon evolution	Canyon length (m)
Joint density in joint set zone—linear decrease in density from center	Similar to main model, with final canyon having flanks less orthogonal to the escarpment	370
Joint density in joint set zone—uniform distribution	Similar to main model, with more spatially uniform failure across the escarpment and a less angular head	340
Thickness of flowing groundwater zone reduced to 25 m	Similar to main model, with faster failure extending towards the top of the escarpment	300
Basic joint density divided by 5	Similar to main model	310
Basic joint direction rotated by 45°	Similar to main model, but with a more angular head	390
Escarpment slope gradient reduced to 45°	Similar to main model	350

and the basinal sediments. The likelihood of fluid seepage in the Blake, Campeche and Malta Escarpments, either at present or in the past, is therefore high.

Since the three main factors supporting box canyon formation along the Florida Escarpment also occur in the Blake, Campeche and Malta Escarpments, the model for box canyon formation proposed for the Florida Escarpment should also be applicable to these. This may be valid for other carbonate escarpments that have been mapped and studied in less detail. The 3,300 m high Bahama Escarpment, for example, exposes Early to middle Cretaceous platform interior jointed limestones (Cavailhes et al., 2020; Freeman-Lynde et al., 1981) (Figure 2). The escarpment geometry indicates an erosional origin with a retreat of 5 km at its base since the Lower Cretaceous, predominantly by spalling, current erosion, slope failure and dissolution (Freeman-Lynde et al., 1981; Freeman-Lynde & Ryan, 1985; Mullins & Hine, 1989; Schlager et al., 1984; Walles, 1993). Saline water and brines, generated by the dissolution of anhydrite (Chanton et al., 1991), are thought to seep at the base of the Bahama Escarpment (Henderson et al., 1999). The 1,000 m high Apulian Escarpment in the central Mediterranean Sea (Figure 2), on the other hand, comprises Late Cretaceous shallow water limestones that feature box canyons (Bosellini, 2002; Groupe Escarmed, 1983; Volpi et al., 2011). Other similar features occur offshore Grand Banks, which comprises a Jurassic to Cretaceous 5-km-high escarpment hosting submarine canyons (Ryan & Miller, 1981), the Mazagan Escarpment offshore Morocco (Auzende et al., 1983; Ruellan et al., 1984; Winterer & Hinz, 1984), and offshore northwestern Australia (Veevers, 1974).

A rock fabric conducive to fluid seepage is commonly found in carbonate platforms globally. Syn-depositional fractures, especially margin perpendicular fractures, are widely recognized in carbonate platforms (Cozzi, 2000; Frost & Kerans, 2009; Guidry et al., 2007; Lehner, 1991). Factors leading to their development include gravity, antecedent topography, and tectonics. Recently it has been suggested that such fractures can develop without the influence of regional tectonic stress (Nooitgedacht et al., 2018). Margin parallel fractures are localized around platform margin, suggesting a gravitational driver for the formation of tensile

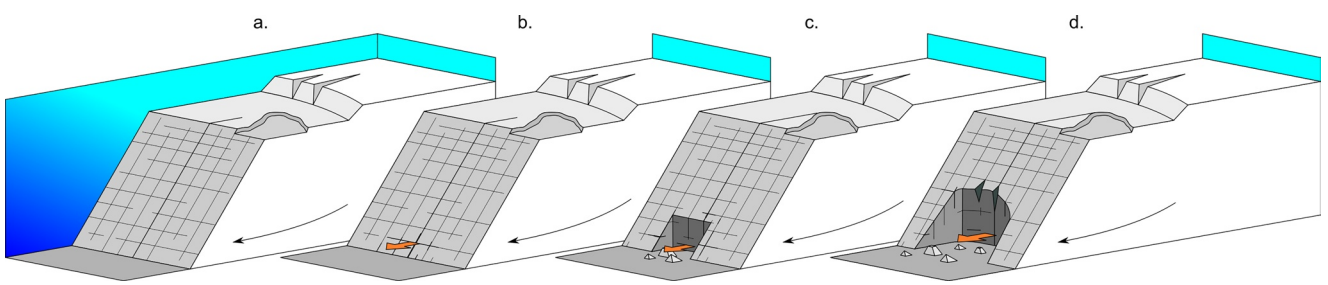

Figure 11. Schematic model for the evolution of a box canyon at the Florida Escarpment derived from the numerical simulations. Arrows are representative of fluid flow (black) and seepage (orange).

stress. Perpendicular fractures, on the other hand, form sub-vertical dikes and fracture corridors. They are a systematic feature in the slopes of flat-topped carbonate platforms and are generated by downslope loading and differential compaction.

5.4.2. General Implications

There are three main general implications associated with our results. First, the location, and possibly geometry/dimension of box canyons, may provide insights into carbonate platform structure, as well as its hydrogeology (e.g., extent of fluid seepage and its fluxes) and the potential occurrence of chemosynthetic communities. This is particularly relevant for the Campeche and Malta Escarpments, which host the highest areas of box canyons per escarpment length (Table 3). Second, the slow development of box canyons at multi-km depth by low frequency head failure suggests that these features do not comprise a significant geohazard. V-shaped canyons are conduits for higher frequency sedimentary flows and they are expected to be more hazardous, especially for submarine cables. With respect to tsunami generation, the highest risk is posed by submarine landslides on ramps, in view of their large area and shallow depths (e.g., Chaytor et al., 2016). Third, the model for box canyon formation in carbonate escarpments may be applicable to other bedrock margins, involving different lithologies (e.g., sandstone) and fluids (meteoric), where similar landforms have been documented, for example, Norwegian margin (Hong et al., 2019; Rise et al., 2013) and SE Australian margin (Mitchell et al., 2007; Varma & Michael, 2012).

6. Conclusions

Based on analyses of multibeam echosounder data from the Blake, Campeche, Malta and Florida Escarpments, and 3-D numerical modeling of the latter, we infer that groundwater plays a key role in the geomorphic evolution of carbonate escarpments. Our main conclusions are the following:

1. Box canyon formation is, in general, a significant erosive process across carbonate escarpments.
2. While v-shaped canyons across the gentler sloping and convex sections of carbonate escarpments likely correspond to bedrock erosion by gravity flows, box canyons are attributed to fluid seepage.
3. 3-D Distinct Element Modeling shows that the initiation and retrogressive evolution of a box canyon can be driven by fluid seeping via joints, which leads to a reduction in rock strength due to fluid pressure (pore and joint fluid pressure) and dissolution, resulting in periodic block failure at the canyon head. The efficacy of these processes was demonstrated using geological, geotechnical and hydraulic parameters from the Florida Escarpment.
4. The modeling reveals that box canyon elongation is promoted by: (a) an exponential distribution of joint density across a joint set zone, (b) perpendicular and parallel orientations of basic joints relative to the escarpment, (c) an increase in the basic joint density, the thickness of the flowing groundwater zone, or the slope gradient of the escarpment. The angularity of the canyon head tends to decrease with a decrease in the basic joint density, or when the distribution of joint density across a joint set zone is uniform. The width of the box canyon is controlled by the width of the joints set zone.
5. The main factors supporting box canyon formation along the base of the Florida Escarpment are: (a) an internal, density-driven fluid circulation system that gives rise to seepage of corrosive fluids at the base of the escarpment, (b) limestone and dolomite outcrops that are susceptible to dissolution, and (c) fabric (joints, faults) that enhances groundwater flow to, and seepage across, the escarpment, and which facilitates fragmentation and failure of rock faces. Since these elements also appear to occur in the Blake, Campeche, and Malta Escarpments, the groundwater model for box canyon formation should be applicable to these escarpments as well.

Data Availability Statement

Multibeam echosounder data from the Blake and Florida Escarpments were downloaded from the National Centres for Environmental Information (https://www.ncei.noaa.gov/maps/bathymetry/). Multibeam echosounder data from the Campeche and Malta Escarpments are available from Marine Geoscience Data system (https://www.marine-geo.org/tools/new_search/index.php?&output_info_all=on&entry_id=FK007) and EMODnet Bathymetry (https://portal.emodnet-bathymetry.eu/), respectively.

Acknowledgments
This project has received funding from the European Research Council (ERC) (grant agreement No 677898 (MARCAN)) and Marie Skłodowska-Curie Actions (grant agreement No 101003394 (RhodoMalta)) under the European Union's Horizon 2020 research and innovation programme, Marie Curie Career Integration Grant PCIG13-GA-2013-618149 (SCARP) under the 7th European Community Framework Programme, the Fulbright Visiting Scholar Program, and the David and Lucile Packard Foundation. We are indebted to the Schmidt Ocean Institute for new Campeche and Florida Escarpment data, and Dave Caress, Eve Lundsten, and Krystle Anderson for compiling data from multiple sources. Open access funding enabled and organized by Projekt DEAL.

References

Amidon, W. H., & Clark, A. C. (2015). Interaction of outburst floods with basaltic aquifers on the Snake River Plain: Implications for Martian canyons. *GSA Bulletin*, *127*(5–6), 688–701. https://doi.org/10.1130/b31141.1

Applin, P. L., & Applin, E. R. (1965). The Comache series and associated rocks in the subsurface in central and south Florida. *U.S. Geological Survey Professional Papers*, *447*, 86.

Argnani, A., & Bonazzi, C. (2005). Malta Escarpment fault zone offshore eastern Sicily: Pliocene-Quaternary tectonic evolution based on new multichannel seismic data. *Tectonics*, *24*, TC4009. https://doi.org/10.1029/2004tc001656

Arthur, M. A., Von Rad, U., Cornfold, C., McCoy, F. W., & Sarnthein, M. (1979). *Evolution and sedimentary history of the Cape Bojador continental margin, northwestern Africa* (Vol. *47*, pp. 773–816). Initial reports of the deep sea drilling project.

Auzende, J. M., Von Rad, U., Diju-Duval, B., Cepek, P., Cousin, M., Dostman, H., et al. (1983). Structure and stratigraphy of Mazagan (El Jadida) escarpment (West Morocco): First results of CYAMAZ diving campaign. *Nature*, *305*, 698–701.

Ball, M. M., Martin, R. G., Foote, R. Q., Leinback, J., Applegate, A. V., Nichols, D., et al. (1988). *Seismic and subsurface structure and stratigraphy of the western Florida shelf*.

Bandis, S. C., Lumsdent, A. C., & Barton, N. R. (1983). Fundamentals of rock joint deformation. *International Journal of Rock Mechanics and Mining Sciences*, *20*(6), 249–268. https://doi.org/10.1016/0148-9062(83)90595-8

Benson, W. E., Sheridan, R. E., Enos, P., Freeman, T., Gradstein, F., Murdmaa, I. O., et al. (1978). Site 392; south rim of Blake Nose. In W. E. Benson, R. E. Sheridan, L. Pastouret, P. Enos, T. Freeman, I. O. Murdmaa, P. Worstell, F. Gradstein, R. R. Schmidt, F. M. Weaver, & D. H. Stuermer (Eds.), *Initial reports of the deep sea drilling project; volume XLIV covering Leg 44 of the cruises of the drilling vessel Glomar Challenger; Norfolk, Virginia to Norfolk, Virginia, August-September 1975* (pp. 337–393). DSDP Deep Sea Drilling Project.

Biju-Duval, B., Morel, Y., Baudrimont, A., Bizon, G., Bizon, J. J., Borsetti, A. M., et al. (1982). Donnees nouvelles sur le marges du Bassin Ionien profon (Mediterranee Orientale): Resultats des campagnes ESCARMED. *Revue de Institut Francais du Petrole*, *37*(6), 713–732. https://doi.org/10.2516/ogst:1982036

Biot, M. A. (1941). General theory of three-dimensional consolidation. *Journal of Applied Physics*, *12*, 144–164. https://doi.org/10.1063/1.1712886

Bird, D. E., Burke, K., Hall, S. A., & Casey, J. F. (2005). Gulf of Mexico tectonic history: Hotspot tracks, crustal boundaries, and early salt distribution. *AAPG Bulletin*, *89*(3), 311–328. https://doi.org/10.1306/10280404026

Bishop, W. F., & Debono, G. (1996). The hydrocarbon geology of southern offshore Malta and surrounding regions. *Journal of Petroleum Geology*, *19*(2), 129–160. https://doi.org/10.1111/j.1747-5457.1996.tb00422.x

Bosellini, A. (2002). Dinosaurs "re-write" the geodynamics of the eastern Mediterranean and the paleogeography of the Apulia Platform. *Earth-Science Reviews*, *59*, 211–234. https://doi.org/10.1016/s0012-8252(02)00075-2

Bralower, T. J., Paull, C. K., & Leckie, R. M. (1998). The Cretaceous-Tertiary boundary cocktail: Chicxulub impact triggers margin collapse and extensive sediment gravity flows. *Geology*, *26*(4), 331–334. https://doi.org/10.1130/0091-7613(1998)026<0331:tctbcc>2.3.co;2

Brook, M., Kirkbride, M., & Brock, B. (2006). Quantified time scale for glacial valley cross-profile evolution in alpine mountains. *Geology*, *34*, 637–640. https://doi.org/10.1130/g22700.1

Brooks, G. R., Doyle, L. J., & McNeillie, J. I. (1986). *A massive carbonate gravity-flow intercalated in the Lower Mississippi Fan* (Vol. *96*, pp. 541–546). Initial reports of the deep sea drilling project.

Bryant, W. R., Meyerhoff, A. A., Brown, N. K., Furrer, M., Pyle, T., & Antoine, J. W. (1969). Escarpment reef trends, and diapiric structures, eastern Gulf of Mexico. *Bulletin of the American Association of Petroleum Geologists*, *53*, 2506–2542. https://doi.org/10.1306/5d25c971-16c1-11d7-8645000102c1865d

Caine, J. S., Evans, J. P., & Forster, C. B. (1996). Fault zone architecture and permeability structure. *Geology*, *24*, 1025–1028. https://doi.org/10.1130/0091-7613(1996)024<1025:fzaaps>2.3.co;2

Cappa, F., Guglielmi, Y., Turqvist, J., Tsang, C. F., & Thoraval, A. (2008). Estimation of fracture flow parameters through numerical analysis of hydromechanical pressure pulses. *Water Resources Research*, *44*, W11408. https://doi.org/10.1029/2008wr007015

Carannante, G., D'Argenio, B., Marsella, E., Neumann, A. C., & Paull, C. K. (1988). *Scarpate Mesozoiche dell'Appennino Meridionale: Confront0 con la scarpata della Florida Occidentale*. Paper presented at the 74° Congresso della Societa' Geological Italiana.

Casero, P., Cita, M. B., Croce, M., & De Micheli, A. (1984). Tentative di interpretazione evolutiva della scarpata di Malta basata su dati geologici e geofisic. *Memorie della Societa` Geologica Italiana*, *27*, 233–253.

Catalano, R., Franchino, A., Merlini, S., & Sulli, A. (2000). A crustal section from Eastern Algerian basin to the Ionian ocean (Central Mediterranean). *Memorie della Societa` Geologica Italiana*, *55*, 71–85.

Cavailhes, T., Gillet, H., Guiastrennec-Faugas, L., Mulder, T., & Hanquiez, V. (2020). The abyssal giant pockmarks of the Black Bahama Escarpment: Relations between structures, fluids and carbonate physiography. *Solid Earth Discussions*, 1–30.

Cernobori, L., Hirn, A., McBride, J. H., Nicolich, R., Petronio, L. R. M., & Romanelli, M. (1996). Crustal image of the Ionian Basin and its Calabrian margins. *Tectonophysics*, *264*, 175–189. https://doi.org/10.1016/s0040-1951(96)00125-4

Chanton, J. P., Martens, C. S., & Paull, C. K. (1991). Control of pore-water chemistry at the base of the Florida escarpment by processes within the platform. *Nature*, *349*, 229–231. https://doi.org/10.1038/349229a0

Chanton, J. P., Martens, C. S., Paull, C. K., & Coston, J. A. (1993). Sulfur isotope and porewater geochemistry of Florida escarpment seep sediments. *Geochimica et Cosmochimica Acta*, *57*, 1253–1266. https://doi.org/10.1016/0016-7037(93)90062-2

Chaytor, J. D., Geist, E. L., Paull, C. K., Caress, D. W., Gwiazda, R., Fucugauchi, J. U., & Vieyra, M. R. (2016). Source characterization and tsunami modeling of submarine landslides along the Yucatán Shelf/Campeche Escarpment, Southern Gulf of Mexico. *Pure and Applied Geophysics*, *173*(12), 4101–4116. https://doi.org/10.1007/s00024-016-1363-3

Cita, M. B., Benelli, F., Bigioggero, B., Chezar, H., Colombo, A., Fantini Sestini, N., et al. (1980). Contribution to the geological exploration of the Malta Escarpment (eastern Mediterranean). *Rivista Italiana di Paleontologia e Stratigrafia*, *86*(2), 316–356.

Commeau, R. F., Paull, C. K., Commeau, J. A., & Poppe, L. J. (1987). Chemistry and mineralogy of pyrite-enriched sediments at a passive margin sulfide brine seep: Abyssal Gulf of Mexico. *Earth and Planetary Science Letters*, *82*(1–2), 62–74. https://doi.org/10.1016/0012-821x(87)90107-5

Corso, W. P., Austin, J. A., & Buffler, R. T. (1989). The Early Cretaceous platform off northwest Florida: Controls on morphologic development of carbonate margins. *Marine Geology*, *86*, 1–14. https://doi.org/10.1016/0025-3227(89)90014-5

Corso, W. P., & Buffler, R. T. (1985). Seismic stratigraphy of lower Cretaceous platforms and margins, eastern Gulf of Mexico. *AAPG Bulletin*, *69*, 246. https://doi.org/10.1306/ad461ddb-16f7-11d7-8645000102c1865d

Cozzi, A. (2000). Synsedimentary tensional features in Upper Triassic shallow-water platform carbonates of the Carnian Prealps (northern Italy) and their importance as palaeostress indicators. *Basin Research*, *12*, 133–146. https://doi.org/10.1046/j.1365-2117.2000.00117.x

Cundall, P. A., & Strack, O. D. L. (1979). A discrete numerical model for granular assemblies. *Géotechnique*, *29*(1), 47–65. https://doi.org/10.1680/geot.1979.29.1.47

Denne, R. A., Scott, E. D., Eickhoff, D. P., Kaiser, J. S., Hill, R. J., & Spaw, J. M. (2013). Massive Cretaceous-Paleogene boundary deposit, deep-water Gulf of Mexico: New evidence for widespread Chicxulub-induced slope failure. *Geology*, *41*, 983–986. https://doi.org/10.1130/g34503.1

Dillon, W. P., Paull, C. K., Buffler, R. T., & Fail, J. P. (1979). Structure and development of the Southeast Georgia Embayment and northern Blake Plateau, preliminary analysis. In J. S. Watkins, L. Montadert, & P. W. Dickerson (Eds.), *Geological and geophysical investigations of continental margins* (Vol. *29*, pp. 27–41). AAPG Memoir.

Dillon, W. P., Paull, C. K., & Gilbert, L. E. (1985). History of the Atlantic continental margin off Florida: The Blake Plateau. In C. W. Poag (Ed.), *Geological evolution of the United States Atlantic margin* (pp. 189–216). Van Nostrand Reinhold Company.

Dillon, W. P., & Popenoe, P. (1988). The Blake Plateau Basin and Carolina Trough. In R. E. Sheridan, & J. A. Grow (Eds.), *The geology of North America* (Vol. *I-2*, pp. 291–328) Geological Society of America.

Dillon, W. P., Risch, J. S., Scanlon, K. M., Valentine, P. C., & Huggett, Q. J. (1993). Ancient crustal fractures control the location and size of collapsed blocks at the Blake Escarpment, east of Florida. *U.S. Geological Survey Bulletin*, 54-59.

Dillon, W. P., Valentine, P. C., & Paull, C. K. (1987). The Blake Escarpment - A product of erosional processes in the deep ocean. In R. Cooper (Ed.), *Symposium series for undersea research* (Vol. *2*, pp. 177–190). National Oceanic and Atmospheric Administration.

Domenico, P. A., & Schwartz, F. W. (1997). *Physical and chemical hydrogeology*. John Wiley.

Dunne, T. (1980). Formation and controls of channel networks. *Progress in Physical Geography*, *4*, 211–239. https://doi.org/10.1177/030913338000400204

Dunne, T. (1990). Hydrology, mechanics, and geomorphic implications of erosion by subsurface flow. In C. G. Higgins, & D. R. Coates (Eds.), *Groundwater geomorphology: The role of subsurface water in Earth-surface processes and landforms* (Vol. *252*, pp. 1–28). Special Paper Geological Society of America. https://doi.org/10.1130/spe252-p1

Fanning, K. A., Byrne, R. H., Breland, J. A., Bettzer, P. R., Moore, S. W., Elsinger, R. J., & Pyle, T. E. (1981). Geothermal springs of the west Florida continental shelf: Evidence for dolomitization and radionuclide enrichment. *Earth and Planetary Science Letters*, *52*, 345–354. https://doi.org/10.1016/0012-821x(81)90188-6

Feeley, M. H., Buffler, R. T., & Bryan, W. R. (1985). Depositional units and growth patterns of the Mississippi Fan. In A. H. Bouma, W. R. Normark, & N. E. Barnes (Eds.), *Submarine fans and related turbidite systems* (pp. 253–257). Springer. https://doi.org/10.1007/978-1-4612-5114-9_37

Finetti, I. (1982). Structure, stratigraphy and evolution of the central Mediterranean. *Bollettino di Geofisica Teorica e Applicata*, *24*, 274–315.

Freeman-Lynde, R. P. (1983). Cretaceous and Tertiary samples dredged from the Florida Escarpment, eastern Gulf of Mexico. *Gulf Coast Association of Geological Studies Transactions*, *33*, 91–99.

Freeman-Lynde, R. P., Cita, M. B., Jadoul, F., Miller, E. L., & Ryan, W. B. F. (1981). Marine geology of the Bahama Escarpment. *Marine Geology*, *44*(1–2), 119–156. https://doi.org/10.1016/0025-3227(81)90115-8

Freeman-Lynde, R. P., & Ryan, W. B. F. (1985). Erosional modification of Bahama Escarpment. *Geological Society of America Bulletin*, *96*(4), 481–494. https://doi.org/10.1130/0016-7606(1985)96<481:emobe>2.0.co;2

Frost, E. L., & Kerans, C. (2009). Platform-margin trajectory as a control on syndepositional on syndepositional fracture patterns, Canning Basin, Western Australia. *Journal of Sedimentary Research*, *79*, 44–55. https://doi.org/10.2110/jsr.2009.014

Garcia-Rios, M., Luquot, L., Soler, J. M., & Cama, J. (2015). Influence of the flow rate on dissolution and precipitation features during percolation of CO_2-rich sulfate solutions through fractured limestone samples. *Chemical Geology*, *414*, 95–108. https://doi.org/10.1016/j.chemgeo.2015.09.005

Gatt, P. A. (2012). *Carbonate facies, depositional sequences and tectonostratigraphy of the Palaeogene Malta Platform*. (PhD). University of Durham.

Gerber, T. P., Amblas, D., Wolinsky, M. A., Pratson, L. F., & Canals, M. (2009). A model for the long-profile shape of submarine canyons. *Journal of Geophysical Research*, *114*, F03002. https://doi.org/10.1029/2008jf001190

Given, M. M. (1977). Mesozoic and early Cenozoic geology of offshore Nova Scotia. *Bulletin of Canadian Petroleum Geology*, *25*, 63–91.

Goldflam, P., Henz, K., Weigel, W., & Wissmann, G. (1980). *Some Features of the Northwest African Margin and Magnetic Quiet Zone* (Vol. *294*, pp. 87–95). Philosophical Transaction of the Royal Society.

Goodman, R. E. (1970). *Deformation of joints*. Paper presented at the Determination of the in-situ modulus of deformation of rock, Denver.

Grasso, M. (1993). Pleistocene structures along the Ionian side of the Hyblean Plateau (SE Sicily): Implications for the tectonic evolution of the Malta Escarpment. In M. D. Max, & P. Colantoni (Eds.), *Geological development of the Sicilian-Tunisian platform* (Vol. *58*, pp. 49–54). UNESCO.

Groupe Escarmed. (1983). Exemples de se´dimentation condensee sur les escarpements de la Mer Ionienne (Mediterranee orientale). Observatios a` partir du submersible 'Cyana'. *Revue de l'Institut Francais du Petrole*, *38*, 427–438.

Guidry, S. A., Grasmueck, M., Carpenter, D. G., Gombos, A. M., Bachtel, S. L., & Viggiano, D. A. (2007). Karst and Early fracture networks in Carbonates, Turks and Caicos Islands, British West Indies. *Journal of Sedimentary Research*, *77*, 508–524. https://doi.org/10.2110/jsr.2007.052

Gulick, S. P. S., Christeson, G. L., Barton, P. J., Grieve, R. A. F., Morgan, J. V., & Urrutia-Fucugauchi, J. (2013). Geophysical characterization of the Chicxulub impact crater. *Reviews of Geophysics*, *51*, 31–52. https://doi.org/10.1002/rog.20007

Gutscher, M.-A., Dominguez, S., de Lepinay, B. M., Pinheiro, L., Gallais, F., Babonneau, N., et al. (2016). Tectonic expression of an active slab tear from high-resolution seismic and bathymetric data offshore Sicily (Ionian Sea). *Tectonics*, *35*(1), 39–54. https://doi.org/10.1002/2015tc003898

Hanshaw, B. B., & Back, W. (1980). Chemical mass wasting of the northern Yucatan Penninsula by ground-water dissolution. *Geology*, *8*, 222–224. https://doi.org/10.1130/0091-7613(1980)8<222:cmotny>2.0.co;2

Heath, R. A. (1985). A review of the physical oceanography of the seas around New Zealand - 1982. *New Zealand Journal of Marine & Freshwater Research*, *19*, 79–124. https://doi.org/10.1080/00288330.1985.9516077

Hecker, B. (1985). Fauna from a cold sulfur-seep in the Gulf of Mexico: Comparison with hydrothermal vent communities and evolutionary implications. *Bulletin of the Biological Society of Washington*, *6*, 465–474.

Henderson, G. M., Slowey, N. C., & Haddad, G. A. (1999). Fluid flow through carbonate platforms: Constraints from 234U/238U and Cl- in Bahamas pore-waters. *Earth and Planetary Science Letters*, *169*, 99–111. https://doi.org/10.1016/s0012-821x(99)00065-5

Holmes, C. M. (1985). Accretion of the south Florida Platform, Late Quaternary development. *Bulletin of the American Association of Petroleum Geologists*, *69*, 149–160. https://doi.org/10.1306/ad461c69-16f7-11d7-8645000102c1865d

Hong, W.-L., Lepland, A., Himmler, T., Kim, J.-H., Chand, S., Sahy, D., et al. (2019). Discharge of meteoric water in the Eastern Norwegian Sea since the Last Glacial Period. *Geophysical Research Letters*, *46*(14), 8194–8204. https://doi.org/10.1029/2019gl084237
Hudec, M., & Norton, I. O. (2019). Upper Jurassic structure and evolution of the Yucatán and Campeche subbasins, southern Gulf of Mexico. *American Association of Petroleum Geologists Bulletin*, *103*(5), 1133–1151. https://doi.org/10.1306/11151817405
Hughes, J. D., Vacher, H. L., & Sanford, W. E. (2007). Three-dimensional flow in the Florida platform: Theoretical analysis of Kohout convection at its type locality. *Geology*, *35*(7), 663–666. https://doi.org/10.1130/g23374a.1
Hummel, N., & Müller, T. M. (2009). Microseismic signatures of non-linear pore-fluid pressure diffusion. *Geophysical Journal International*, *179*(3), 1558–1565. https://doi.org/10.1111/j.1365-246x.2009.04373.x
Jaeger, J. C., Cook, N. G. W., & Zimmermann, R. W. (2007). *Fundamentals of rock mechanics*. Blackwell.
Klitgord, K. D., Popenoe, P., & Scholten, H. (1984). Florida: A Jurassic transform plate boundary. *Journal of Geophysical Research*, *89*(B9), 7753–7772. https://doi.org/10.1029/jb089ib09p07753
Klitgord, K. D., & Schouten, H. (1986). Plate kinematics of the central Atlantic. In P. R. Vogt & B. E. Tucholke (Eds.), *The geology of North America* (Vol. M, pp. 351–358). Geological Society of America.
Kohl, B. (1985). Biostratigraphy and sedimentation rates of the Mississippi Fan. In A. H. Bouma, W. R. Normark, & N. E. Barnes (Eds.), *Submarine fans and related turbidity systems* (pp. 267–273). Springer. https://doi.org/10.1007/978-1-4612-5114-9_39
Kohout, F. A. (1965). A hypothesis concerning cyclic flow of salt water related to geothermal heating in the Floridan aquifer. *New York Academy of Sciences Transactions*, *28*, 249–271. https://doi.org/10.1111/j.2164-0947.1965.tb02879.x
Koumantakis, J., & Sachpazis, C. I. (1989). The engineering geological properties of the Triassic dolomite of the Stefani area (Greece) in relation to its suitability in skid resistant pavement surface construction. *Bulletin of the International Association of Engineering Geology*, *33*, 103–107.
Laity, J. E., & Malin, M. C. (1985). Sapping processes and the development of theater-headed valley networks in the Colorado Plateau. *Geological Society of America Bulletin*, *96*, 203–217. https://doi.org/10.1130/0016-7606(1985)96<203:spatdo>2.0.co;2
Lamb, M. P., Dietrich, W. E., Aciego, S. M., DePaolo, D. J., & Manga, M. (2008). Formation of Box Canyon, Idaho, by megaflood: Implications for seepage erosion on Earth and Mars. *Science*, *320*, 1067–1070. https://doi.org/10.1126/science.1156630
Lamb, M. P., Howard, A. D., Dietrich, W. E., & Perron, J. T. (2007). Formation of amphitheatre-headed valleys by waterfall erosion after large-scale slumping on Hawai'i. *GSA Bulletin*, *119*(7/8), 805–822. https://doi.org/10.1130/b25986.1
Lamb, M. P., Howard, A. D., Johnson, J., Whipple, K. X., Dietrich, W. E., & Perron, J. T. (2006). Can springs cut canyons into rock? *Journal of Geophysical Research*, *111*, E07002. https://doi.org/10.1029/2005je002663
Lamb, M. P., Mackey, B. H., & Farley, K. A. (2014). Amphitheater-headed canyons formed by megaflooding at Malad Gorge, Idaho. *Proceedings of the National Academy of Sciences of the United States of America*, *111*(1), 57–62. https://doi.org/10.1073/pnas.1312251111
Lancelot, Y., & Seibold, E. (1977). *The evolution of the central northeastern Atlantic - Summary of results of DSDP Leg 41* (Vol. *41*, pp. 1215–1245). Initial reports of the deep sea drilling project.
Land, L. A., Paull, C. K., & Spiess, F. N. (1999). Abyssal erosion and scarp retreat: Deep Tow observations of the Blake Escarpment and Blake Spur. *Marine Geology*, *160*(1–2), 63–83. https://doi.org/10.1016/s0025-3227(99)00012-2
Lapotre, M. G. A., & Lamb, M. P. (2018). Substrate control on valley formation by groundwater on Earth and Mars. *Geology*, *46*(6), 531–534. https://doi.org/10.1130/g40007.1
Lehner, B. L. (1991). Neptunian dykes along a drowned carbonate platform margin: An indication for recurrent extensional tectonic activity? *Terra Nova*, *3*, 593–602. https://doi.org/10.1111/j.1365-3121.1991.tb00201.x
Liao, Z., Liu, H., Carpenter, B. M., Marfurt, K. J., & Reches, Z. (2019). Analysis of fault damage zones using three-dimensional seismic coherence in the Anadarko Basin, Oklahoma. *AAPG Bulletin*, *103*(8), 1771–1785. https://doi.org/10.1306/1219181413417207
Lindsay, J. F., Shipley, T. H., & Worzel, J. L. (1975). Role of canyons in the growth of the Campeche Escarpment. *Geology*, *3*(9), 533–536. https://doi.org/10.1130/0091-7613(1975)3<533:rocitg>2.0.co;2
Lobkovsky, A. E., Smith, B. A., Kudrolli, A., Mohrig, D., & Rothman, D. H. (2007). Erosive dynamics of channels incised by subsurface water flow. *Journal of Geophysical Research*, *112*, F03S12. https://doi.org/10.1029/2006jf000517
Locker, S. D., & Buffler, R. T. (1983). Comparison of Lower Cretaceous carbonate shelf margins, northern Campeche Escarpment and northern Florida Escarpment, Gulf of Mexico. *American Association of Petroleum Geologists Bulletin*, *15*. 2.2.3-123–2.2.3-128.
Luo, W., & Howard, A. D. (2008). Computer simulation of the role of groundwater seepage in forming Martian valley networks. *Journal of Geophysical Research*, *113*, E05002. https://doi.org/10.1029/2007je002981
Manheim, F. T. (1967). Evidence for submarine discharge of water on the Atlantic continental slope of the southern United States, and suggestions for further research. *Transactions of the New York Academy of Science*, *29*, 839–853. https://doi.org/10.1111/j.2164-0947.1967.tb02825.x
Manheim, F. T., & Horn, M. K. (1968). Composition of deeper subsurface waters along the Atlantic continental margin. *Southeastern Geology*, *9*, 215–236.
Maricic, A., Starcevic, K., & Barudyija, U. (2018). Physical and mechanical properties of dolomites related to sedimentary and diagenetic features – Case study of the Upper Triassic dolomites from the Medvednica and Samobor Mts., NW Croatia. *The Mining-Geological-Petroleum Engineering Bulletin*, *33*(3), 33–44.
Martens, C. S., Chanton, J. P., & Paull, C. K. (1991). Biogenic methane from abyssal brine seeps at the base of the Florida Escarpment. *Geology*, *19*, 851–854. https://doi.org/10.1130/0091-7613(1991)019<0851:bmfabs>2.3.co;2
McVay, M., Song, X., Wasman, S., Nguyen, T., & Wang, K. (2019). *Strength envelopes for Florida rock and intermediate geomaterials*.
Micallef, A., Camerlenghi, A., Georgiopoulou, A., Garcia-Castellanos, D., Gutscher, M.-A., Lo Iacono, C., et al. (2019). Geomorphic evolution of the Malta Escarpment and implications for the Messinian evaporative drawdown in the eastern Mediterranean Sea. *Geomorphology*, *327*, 264–283. https://doi.org/10.1016/j.geomorph.2018.11.012
Micallef, A., Georgiopoulou, A., Mountjoy, J., Huvenne, V., Lo Iacono, C., Le Bas, T., et al. (2016). Outer shelf seafloor geomorphology along a carbonate escarpment: The eastern Malta Plateau, Mediterranean Sea. *Continental Shelf Research*, *131*, 12–27. https://doi.org/10.1016/j.csr.2016.11.002
Micallef, A., Marchis, R., Saadatkhah, N., Pondthai, P., Everett, M. E., Avram, A., et al. (2021). Groundwater erosion of coastal gullies along the Canterbury coast (New Zealand): A rapid and episodic process controlled by rainfall intensity and substrate variability. *Earth Surface Dynamics*, *8*, 1–18. https://doi.org/10.5194/esurf-9-1-2021
Micallef, A., Mountjoy, J., Barnes, P. M., Canals, M., & Lastras, G. (2014). Geomorphic response of submarine canyons to tectonic activity: Insights from the Cook Strait canyon system, New Zealand. *Geosphere*, *10*(5), 905–929. https://doi.org/10.1130/ges01040.1
Micallef, A., Ribó, M., Canals, M., Puig, P., Lastras, G., & Tubau, X. (2014). Space-for-time substitution and the evolution of a submarine canyon–channel system in a passive progradational margin. *Geomorphology*, *221*, 34–50. https://doi.org/10.1016/j.geomorph.2014.06.008

Mitchell, J. K., Holdgate, G. R., Wallace, M. W., & Gallagher, S. J. (2007). Marine geology of the Quaternary Bass Canyon system, southeast Australia: A cool-water carbonate system. *Marine Geology*, *237*, 71–96. https://doi.org/10.1016/j.margeo.2006.10.037

Mitchell, N. C. (2005). Interpreting long-profiles of canyons in the USA Atlantic continental slope. *Marine Geology*, *214*, 75–99. https://doi.org/10.1016/j.margeo.2004.09.005

Mitchell, N. C. (2014). Bedrock erosion by sedimentary flows in submarine canyons. *Geosphere*, *10*(5), 892–904. https://doi.org/10.1130/ges01008.1

Morgan, J., Warner, M., Chicxulub Working Group, Brittan, J., Buffler, R., Camargo, A., et al. (1997). Size and morphology of the Chicxulub impact crater. *Nature*, *390*, 472–476. https://doi.org/10.1038/37291

Mullins, H. T., Gardulski, A. F., Hinckley, E. J., & Hine, A. C. (1988). The modern carbonate ramp slope of Central West Florida. *Journal of Sedimentary Petrology*, *58*(2), 273–290. https://doi.org/10.1306/212f8d73-2b24-11d7-8648000102c1865d

Mullins, H. T., & Hine, A. C. (1989). Scalloped bank margins: Beginning of the end for carbonate platforms? *Geology*, *17*(1), 30–33. https://doi.org/10.1130/0091-7613(1989)017<0030:sbmbot>2.3.co;2

Nagihara, S. (1996). Seepage-induced erosion of submarine carbonate escarpments: A numerical simulation. *Earth and Planetary Science Letters*, *144*(1–2), 263–271. https://doi.org/10.1016/0012-821x(96)00162-8

Neumann, A. C. (1966). Observations on coastal erosion in Bermuda and measurement of boring rates of the sponge *Cliona limpa*. *Limnology and Oceanography*, *2*, 92–108. https://doi.org/10.4319/lo.1966.11.1.0092

Nguyen, T. (2020). *Strength envelopes for Florida rock and intermediate geomaterials*. (PhD). University of Florida.

Nicolich, R., Laigle, M., Hirn, A., Cernobori, L., & Gallart, J. (2000). Crustal structure of the Ionian margin of Sicily: Etna volcano in the frame of regional evolution. *Tectonophysics*, *329*, 121–139. https://doi.org/10.1016/s0040-1951(00)00192-x

Nooitgedacht, C. W., Kleipool, L. M., Andeweg, B., Reolid, J., Betzler, C., Lindhorst, S., & Reijmer, J. J. G. (2018). New insights in the development of syn-depositional fractures in rimmed flat-topped carbonate platforms, Neogene carbonate complexes, Sorbas Basin, SE Spain. *Basin Research*, *30*(S1), 596–612. https://doi.org/10.1111/bre.12239

Norris, R. D., Kroon, D., & Klaus, A. (1998). Site 1052. *Proceedings of the Ocean Drilling Program, 171B*, 241–359.

Palchik, V. (2019). Simple stress–strain model of very strong limestones and dolomites for engineering practice. *Geomechanics and Geophysics for Geo-Energy and Geo-Resources*, *5*, 345–356. https://doi.org/10.1007/s40948-019-00115-2

Paull, C. K., Caress, D. W., Gwiazda, R., Urrutia-Fucugauchi, J., Rebolledo-Vieyra, M., Lundsten, E., et al. (2014). Cretaceous–Paleogene boundary exposed: Campeche Escarpment, Gulf of Mexico. *Marine Geology*, *357*(0), 392–400. https://doi.org/10.1016/j.margeo.2014.10.002

Paull, C. K., Chanton, J. P., Neumann, A. C., Coston, J. A., Martens, C. S., & Showers, W. (1992). Indicators of methane-derived carbonates and chemosynthetic organic carbon deposits: Examples from the Florida Escarpment. *Palaios*, *7*, 361–375. https://doi.org/10.2307/3514822

Paull, C. K., Commeau, R. F., Curray, J. R., & Neumann, A. C. (1991). Seabed measurements of modern corrosion rates on the Florida escarpment. *Geo-Marine Letters*, *11*(1), 16–22. https://doi.org/10.1007/bf02431050

Paull, C. K., & Dillon, W. P. (1980). Erosional origin of the Blake Escarpment: An alternative hypothesis. *Geology*, *8*, 538–542. https://doi.org/10.1130/0091-7613(1980)8<538:eootbe>2.0.co;2

Paull, C. K., Freeman-Lynde, R. P., Bralower, T. J., Gardemal, J. M., Neumann, A. C., D'Argenio, B., & Marsella, E. (1990). Geology of the strata exposed on the Florida Escarpment. *Marine Geology*, *91*, 177–194. https://doi.org/10.1016/0025-3227(90)90035-i

Paull, C. K., Hecker, B., Commeau, R., Freeman-Lynde, R. P., Neumann, A. C., Corso, W. P., et al. (1984). Biological communities at the Florida Escarpment resemble hydrothermal vent taxa. *Science*, *226*, 965–967. https://doi.org/10.1126/science.226.4677.965

Paull, C. K., & Neumann, A. C. (1987). Continental margin brine seeps: Their geological consequences. *Geology*, *15*(6), 545–548. https://doi.org/10.1130/0091-7613(1987)15<545:cmbstg>2.0.co;2

Paull, C. K., Spiess, E. N., Curray, J. R., & Twichell, D. C. (1988). Morphology of Florida Escarpment chemosynthetic brine seep community sites - Deep-tow, Seabeam and Gloria surveys. *AAPG Bulletin*, *72*, 233.

Paull, C. K., Spiess, F. N., Curry, J. R., & Twichell, D. C. (1990). Origin of Florida Canyon and the role of spring sapping on the formation of submarine box canyons. *Geological Society of America Bulletin*, *102*, 502–515. https://doi.org/10.1130/0016-7606(1990)102<0502:oofcat>2.3.co;2

Paull, C. K., Twichell, D. C., Spiess, F. N., & Curray, J. R. (1991). Morphological development of the Florida Escarpment: Observations on the generation of time transgressive unconformities in carbonate terrains. *Marine Geology*, *101*, 181–201. https://doi.org/10.1016/0025-3227(91)90070-k

Pedley, H. M., Debono, G., & Yeaman, M. (1993). Mesozoic structuring and volcanics along the Pelagian-Ionian boundary: A prelude to foundering of the Ionian Basin. In M. D. Max, & P. Colantoni (Eds.), *UNESCO technical reports in marine science* (Vol. *58*, pp. 81–86).

Pelletier, J. D., & Baker, V. R. (2011). The role of weathering in the formation of bedrock valleys on Earth and Mars: A numerical modeling investigation. *Journal of Geophysical Research*, *116*, E11007. https://doi.org/10.1029/2011je003821

Perry, E., Oliman, G. V., & Wagner, N. (2012). Preliminary investigation of groundwater and surface water geochemistry in Campeche and southern Quintana Roo. In Ú. O. Spring (Ed.), *Water resources in Mexico* (Vol. *7*). Springer. https://doi.org/10.1007/978-3-642-05432-7_6

Plummer, L. N. (1975). Mixing of sea water with calcium carbonate ground water. *Geological Society of America Memoirs*, *142*, 219–236. https://doi.org/10.1130/mem142-p219

Popenoe, P. (1985). *Seismic-stratigraphic studies of sinkholes and the Boulder Zone under the northeastern Florida continental shelf*. Geological Society of America Abstracts with Programs, 17, 129.

Pratson, L. F., Nittrouer, C. A., Wiberg, P. L., Steckler, M. S., Swenson, J. B., Cacchione, D. A., et al. (2009). Seascape evolution on clastic continental shelves and slopes. In C. A. Nittrouer, J. A. Austin, M. E. Field, J. H. Kravitz, J. P. M. Syvitski, & P. L. Wiberg (Eds.), *Continental margin sedimentation: from sediment transport to sequence stratigraphy: IAP special publication* (Vol. *37*, pp. 339–380). Blackwell Publishing.

Reuther, C. (1990). Strike slip generated rifting and recent tectonic stresses on the African foreland (Central Mediterranean region). *Annales Tectonicae*, *4*(2), 120–130.

Reuther, C., Ben-Avraham, Z., & Grasso, M. (1993). Origin and role of major strike-slip transfers during plate collision in the central Mediterranean. *Terra Nova*, *5*, 249–257. https://doi.org/10.1111/j.1365-3121.1993.tb00256.x

Rise, L., Bøe, R., Riis, F., Bellec, V. K., Laberg, J. S., Eidvin, T., et al. (2013). The Lofoten-Vesterålen continental margin, North Norway: Canyons and mass-movement activity. *Marine and Petroleum Geology*, *45*, 134–149. https://doi.org/10.1016/j.marpetgeo.2013.04.021

Rodgers, M., McVay, M., Horhota, D., Sinnreich, J., & Hernando, J. (2018). Assessment of shear strength from measuring while drilling shafts in Florida limestone. *Canadian Geotechnical Journal*, *56*(5), 662–674. https://doi.org/10.1139/cgj-2017-0629

Ruellan, E., Auzende, J. M., & Dostman, H. (1984). Structure and evolution of the Mazagan (El Jadida) plateau and escarpment off central Morocco. *Oceanologica Acta*, 59–72.
Russel, I. C. (1902). Geology and water resources of the Snake River Plains of Idaho. *US Geological Survey Bulletin*, *199*, 1–192.
Ryan, A. J., & Whipple, K. X. (2020). Amphitheatre-headed canyons of Southern Utah: Stratigraphic control of canyon morphology. *Earth Surface Processes and Landforms*, *45*(14), 3607–3622. https://doi.org/10.1002/esp.4987
Ryan, W. B. F., & Miller, E. (1981). Evidence of a carbonate platform beneath Georges Bank. *Marine Geology*, *44*, 213–228. https://doi.org/10.1016/0025-3227(81)90119-5
Sagy, A., Reches, Z., & Roman, I. (2001). Dynamic fracturing: Field and experimental observations. *Journal of Structural Geology*, *23*(8), 1223–1239. https://doi.org/10.1016/s0191-8141(00)00190-5
Scandone, P., Patacca, E., Radoicic, R., Ryan, W. B. F., Cita, M. B., Rawson, M., et al. (1981). Mesozoic and Cenozoic rocks from Malta Escarpment (Central Mediterranean). *American Association of Petroleum Geologists Bulletin*, *65*(7), 1299–1319. https://doi.org/10.1306/03b5949f-16d1-11d7-8645000102c1865d
Scheingross, J. S., & Lamb, M. P. (2017). A mechanistic model of waterfall plunge pool erosion into Bedrock. *Journal of Geophysical Research: Earth Surface*, *122*(11), 2079–2104. https://doi.org/10.1002/2017jf004195
Schlager, W. (1981). The paradox of drowned reefs and carbonate platforms. *Geological Society of America Bulletin*, *92*, 197–211. https://doi.org/10.1130/0016-7606(1981)92<197:tpodra>2.0.co;2
Schlager, W. (2005). *Carbonate Sedimentology and Sequence Stratigraphy* (Vol. *8*).
Schlager, W., Austin, J. A., Corso, W. P., McNulty, C. L., Fluegel, E., Renz, O., & Steinmetz, J. C. (1984). Early Cretaceous platform re-entrant and escarpment erosion in the Bahamas. *Geology*, *12*, 147–150. https://doi.org/10.1130/0091-7613(1984)12<147:ecprae>2.0.co;2
Schlager, W., & Camber, O. (1986). Submarine slope angles, drowning unconformities, and self-erosion of limestone escarpments. *Geology*, *14*(9), 762–765. https://doi.org/10.1130/0091-7613(1986)14<762:ssadua>2.0.co;2
Schlee, J. S., Dillon, W. P., & Grow, J. A. (1979). Structure of the continental slope off the Eastern United States. In L. J. Doyle, & O. H. Pilkey (Eds.), *Geology of continental slopes* (Vol. *27*, pp. 95–117). Society Economic Paleontologists Mineralogists Special Publication. https://doi.org/10.2110/pec.79.27.0095
Schumm, S. A., Boyd, K. F., Wolff, C. G., & Spitz, W. J. (1995). A groundwater sapping landscape in the Florida panhandle. *Geomorphology*, *12*(4), 281–297. https://doi.org/10.1016/0169-555x(95)00011-s
Shaub, F. J. (1984). The internal framework of the southwestern Florida Bank. *Transactions - Gulf Coast Association of Geological Societies*, *34*, 237–245.
Sheridan, R. E. (1981). Comment and reply on 'Erosional origin of the Blake Escarpment: An alternative hypothesis'. *Geology*, *9*, 338–339. https://doi.org/10.1130/0091-7613(1981)9<338:caroeo>2.0.co;2
Sikes, E. L. (1984). *Bioerosion of deep carbonates by macro-endoliths*. (MSc). University of North Carolina.
Singh, M., Rao, K. S., & Ramamurthy, T. (2002). Strength and deformation behaviour of a jointed rock mass. *Rock Mechanics and Rock Engineering*, *35*(1), 45–64. https://doi.org/10.1007/s006030200008
Snow, D. T. (1965). *A parallel plate model of fractured permeable media*. (PhD). University of California.
Speranza, F., Minelli, L., Pignatelli, A., & Chiappini, M. (2012). The Ionian Sea: The oldest in situ ocean fragment of the world? *Journal of Geophysical Research*, *117*, B12101. https://doi.org/10.1029/2012jb009475
Terzaghi, K. (1923). Die berechning der durchla¨ssigkeitziffer des tonesaus dem verlauf spannungserscheinungen. *Wien, Sitzungsberichte, Mathematisch-naturwissenschaftliche Klasse*, *142*(3/4), 125–138.
Twichell, D. C., Dillon, W. P., Paull, C. K., & Kenyon, N. H. (1996). Morphology of carbonate escarpments as an indicator of erosional processes. In J. V. Gardner, M. E. Field, & D. C. Twichell (Eds.), *Geology of the United States seafloor: The view from GLORIA* (pp. 97–108). Cambridge University Press.
Twichell, D. C., Parson, L. M., & Paull, C. K. (1990). Variations in the styles of erosion along the Florida Escarpment, eastern Gulf of Mexico. *Marine and Petroleum Geology*, *7*(3), 253–266. https://doi.org/10.1016/0264-8172(90)90003-y
Twichell, D. C., Paull, C. K., & Parson, L. M. (1991). Terraces on the Florida escarpment: Implications for erosional processes. *Geology*, *19*(9), 897–900. https://doi.org/10.1130/0091-7613(1991)019<0897:totfei>2.3.co;2
Uchupi, E., & Emery, K. O. (1968). The structure of continental margins off Gulf Coast of United States. *AAPG Bulletin*, *52*, 1162–1193. https://doi.org/10.1306/5d25c49f-16c1-11d7-8645000102c1865d
Varma, S., & Michael, K. (2012). Impact of multi-purpose aquifer utilisation on a variable-density groundwater flow system in the Gippsland Basin, Australia. *Hydrogeology Journal*, *20*, 119–134. https://doi.org/10.1007/s10040-011-0800-8
Veevers, J. J. (1974). Western continental margins of Australia. In C. A. Burke, & C. L. Drake (Eds.), *The geology of continental margins* (pp. 605–616). Springer. https://doi.org/10.1007/978-3-662-01141-6_44
Volpi, V., Accettella, D., & Cuppari, A. (2011). Morphological features of the Apennines foreland/accretionary-wedge boundary in the Ionian Sea. *Marine Geophysical Researches*, *32*, 481–492. https://doi.org/10.1007/s11001-011-9140-2
Walles, F. E. (1993). Tectonic and diagenetically induced seal failure within the south-western Great Bahamas Bank. *Marine and Petroleum Geology*, *10*, 14–28. https://doi.org/10.1016/0264-8172(93)90096-b
Wilson, J. E., Chester, J. E., & Chester, F. M. (2003). Microfracture analysis of fault growth and wear processes, Punchbowl Fault, San Andreas system, California. *Journal of Structural Geology*, *25*(11), 1855–1873. https://doi.org/10.1016/s0191-8141(03)00036-1
Wilson, P. A., & Roberts, H. H. (1992). Carbonate-periplatform sedimentation by density flows: A mechanism for rapid off-bank and vertical transport of shallow-water fines. *Geology*, *20*, 713–716. https://doi.org/10.1130/0091-7613(1992)020<0713:cpsbdf>2.3.co;2
Winterer, E. L., & Hinz, K. (1984). *Evolution of the Mazagan continental margin: A synthesis of geophysical and geological data with results of drilling during deep sea drilling project leg 79*. Initial reports of the deep sea drilling project, 79, 893-919.
Witherspoon, P. A., Wang, J. S. Y., Iwai, K., & Gale, J. E. (1980). Validity of cubic law for fluid flow in a deformable rock fracture. *Water Resources Research*, *16*(6), 1016–1024. https://doi.org/10.1029/wr016i006p01016
Worzel, J. L., Bryant, W., Beall, A. O., Dickinson, K., Laury, R., Smith, L. A., et al. (1973). *Site 86*. U.S. Government Printing Office.
Yasar, E., & Erdogan, Y. (2004). Correlating sound velocity with the density, compressive strength and Young's modulus of carbonate rocks. *International Journal of Rock Mechanics and Mining Sciences*, *41*, 871–875. https://doi.org/10.1016/j.ijrmms.2004.01.012